



# Hopf and Generalized Hopf Bifurcations in a Recurrent Autoimmune Disease Model

Wenjing Zhang\* and Pei Yu†  
*Department of Applied Mathematics,  
Western University London,  
Ontario, N6A 5B7, Canada*  
\*wzhan88@yorku.ca  
†pyu@uwo.ca

Received September 2, 2015; Revised October 30, 2015

This paper is concerned with bifurcation and stability in an autoimmune model, which was established to study an important phenomenon — blips arising from such models. This model has two equilibrium solutions, disease-free equilibrium and disease equilibrium. The positivity of the solutions of the model and the global stability of the disease-free equilibrium have been proved. In this paper, we particularly focus on Hopf bifurcation which occurs from the disease equilibrium. We present a detailed study on the use of center manifold theory and normal form theory, and derive the normal form associated with Hopf bifurcation, from which the approximate amplitude of the bifurcating limit cycles and their stability conditions are obtained. Particular attention is also paid to the bifurcation of multiple limit cycles arising from generalized Hopf bifurcation, which may yield bistable phenomenon involving equilibrium and oscillating motion. This result may explain some complex dynamical behavior in real biological systems. Numerical simulations are compared with the analytical predictions to show a very good agreement.

*Keywords:* Autoimmune disease model; stability; Hopf bifurcation; generalized Hopf bifurcation; limit cycle; center manifold; normal form.

## 1. Introduction

Autoimmune diseases arise from an inappropriate immune system in responding against its own cells and tissues, which are normally present in the body. A substantial minority of population, approximately 3% of people in “developed” countries, suffer from over 40 recognized autoimmune diseases [DeFranco *et al.*, 2007], which are often chronic, depleting and fatal. Some autoimmune diseases show recurrent (or blips) behavior, which was found typically in multifocal osteomyelitis [Girschick *et al.*, 2007; Iyer *et al.*, 2011], eczema [Fergusson *et al.*, 1990], subacute discoid lupus erythematosus [Munro, 1963], and psoriasis [Farber *et al.*, 1986]. During recurrent

autoimmune disease, the disease symptoms can disappear spontaneously, but it will occasionally relapse later. Therefore, a profound study on the recurrent dynamics of autoimmune disease is important to obtain a broad understanding of this disease phenomenon.

In immune system, regulatory T (Treg) cells, a subpopulation of T cells, play a crucial role in tolerating the body’s own cells and tissues, and suppress the autoimmune response. Treg cells operate primarily at the site of inflammation. The mechanisms for Treg cells modulating the immune reaction is one of the most intensely studied and debated issues, while “there might be a single key mechanism

---

†Author for correspondence

that has a predominant role”, as Miyara and Sakaguchi pointed out in [Miyara & Sakaguchi, 2007]. Here, we adopt two mechanisms proposed in a general autoimmune disease model by Alexander and Wahl [2011]. One mechanism is that Treg cells suppress directly on professional antigen presenting cells (pAPCs), which play a vital role in activating naive T cells, and remove pAPCs permanently. The other mechanism is that the Treg cells directly reduce and remove the peripheral auto-reactive effector T cells, which have antigen receptors specific to self-antigens and ready to attack host cells. Phenotypic analysis shows that Treg cells subset is heterogeneous [Sakaguchi *et al.*, 2010] in the expression of HLA-DR, which identifies a terminally differentiated subpopulation of Treg cells with HLA-DR<sup>+</sup>, called terminal Treg cells. The terminal Treg cells are generated from natural Treg cells proliferation [Sakaguchi *et al.*, 2010], while suppressing more efficiently and tend to be apoptotic much faster than the natural Treg cells. The following mathematical model was established to model the Treg cells activity in modulating the immune response [Zhang *et al.*, 2014],

$$\begin{aligned} \dot{A} &= \alpha E - \sigma_1(R_n + dR_d)A - b_1A - \mu_A A, \\ \dot{R}_n &= (\pi_3 E + \beta)A - \mu_n R_n - \xi R_n, \\ \dot{R}_d &= c\xi R_n - \mu_d R_d, \\ \dot{E} &= \lambda_E A - \sigma_3(R_n + dR_d)E - b_3 E - \mu_E E, \end{aligned} \tag{1}$$

where the state variables  $A$ ,  $R_n$ ,  $R_d$  and  $E$  represent the population of the mature pAPCs, the activated natural Treg cells specific for antigen of interest, terminally differentiated Treg cells, and the active auto-reactive effector T cells with specific antigen of interest. The pAPCs are activated at a rate of  $\alpha E$  by uptaking self-antigen, which is generated by effector T cells attacking body cells. The relation between effector T cells and self-antigen is linear under quasi-steady state assumption. The pAPCs are suppressed by the Treg cells with specific antigen of interest at a rate of  $\sigma_1(R_n + dR_d)A$ , where  $d$  is the ratio of suppressive effectiveness between the natural Treg cells and terminally differentiated Treg cells, while the Treg cells with other specificities and therapy can also suppress pAPCs at a rate of  $b_1$ . The natural Treg cells are activated with interaction of the pAPCs in the presence of IL-2 which is generated by the effector T cells at a rate of  $\pi_3 E$ , and by other sources like dendritic cells (DCs) [Field

*et al.*, 2007; Scheffold *et al.*, 2005; Scheffold *et al.*, 2007] at a rate of  $\beta$ , and thus the natural Treg cells generation rate is  $(\pi_3 E + \beta)A$ . The activated natural Treg cells may undergo further differentiation and proliferation [Sakaguchi *et al.*, 2010] at a rate of  $\xi$  and give birth to terminally differentiated Treg cells at a rate of  $c\xi R_n$ . The vicious effector T cells are activated by the pAPCs bearing a specific antigen receptor, at a rate of  $\lambda_E A$ , and are suppressed by the Treg cells with specific antigen of interest at a rate of  $\sigma_3(R_n + dR_d)E$ , and the Treg cells with other specificities and therapy at a rate of  $b_3 E$ . The death rates of the pAPCs, natural Treg cells, terminally differentiated Treg cells, and effector T cells are  $\mu_A$ ,  $\mu_n$ ,  $\mu_d$ , and  $\mu_E$ , respectively.

It has been shown in [Zhang *et al.*, 2014] that all solutions of (1) are non-negative, if the initial conditions are taken non-negative, and they are bounded. Moreover, a detailed analysis on the stability of equilibrium solutions is also given in [Zhang *et al.*, 2014]. Thus, in this paper, we will focus on the nonlinear study of model (1), in particular on Hopf and generalized Hopf bifurcations, giving rise to multiple limit cycles bifurcating from the disease equilibrium. The rest of the paper is organized as follows. In the next section, we provide a brief summary on the linear analysis of system (1), and find the transcritical and Hopf bifurcations from the equilibrium solutions. Then, in Sec. 3, we devote to nonlinear analysis and focus on Hopf bifurcation. Center manifold theory and normal form theory will be used to find the approximate solution of limit cycles and determine their stability. In Sec. 4, we present a study on generalized Hopf bifurcation, showing that at least two small-amplitude limit cycles can bifurcate from the disease equilibrium. Numerical simulations are given in Sec. 5 to show the good agreement between simulations and analytical predictions. Finally, the conclusion is drawn in Sec. 6.

## 2. Equilibrium Solutions, Stability and Bifurcation: Linear Analysis

In order to consider stability of equilibrium solutions of model (1), we first present certain results and formulas for general systems. Consider the general nonlinear differential system:

$$\begin{aligned} \dot{\mathbf{x}} &= \mathbf{f}(\mathbf{x}, \boldsymbol{\mu}), \quad \mathbf{x} \in \mathbf{R}^n, \quad \boldsymbol{\mu} \in \mathbf{R}^m, \\ \mathbf{f} &: \mathbf{R}^{n+m} \mapsto \mathbf{R}^n, \end{aligned} \tag{2}$$

where the dot denotes differentiation with respect to time  $t$ ;  $\mathbf{x}$  and  $\boldsymbol{\mu}$  are the  $n$ -dimensional state variable and  $m$ -dimensional parameter variable, respectively. It is assumed that the nonlinear function  $\mathbf{f}(\mathbf{x}, \boldsymbol{\mu})$  is analytic with respect to  $\mathbf{x}$  and  $\boldsymbol{\mu}$ . Suppose that the equilibrium solutions of Eq. (2) are given in the form of  $\mathbf{x}_e = \mathbf{x}_e(\boldsymbol{\mu})$ , which are determined from  $\mathbf{f}(\mathbf{x}, \boldsymbol{\mu}) = 0$ . To find the stability of  $\mathbf{x}_e$ , evaluating the Jacobian of system (2) at  $x = \mathbf{x}_e(\boldsymbol{\mu})$  yields  $\mathbf{J}(\boldsymbol{\mu}) = D_{\mathbf{x}}\mathbf{f}|_{x=\mathbf{x}_e(\boldsymbol{\mu})}$ . If all eigenvalues of  $\mathbf{J}(\boldsymbol{\mu})$  have nonzero real parts, then the system is said to be hyperbolic and no complex dynamics exists in the vicinity of the equilibrium solution. If at some point  $\boldsymbol{\mu} = \boldsymbol{\mu}_c$ , at least one of the eigenvalues of  $\mathbf{J}(\boldsymbol{\mu})$  has zero real part, then  $\boldsymbol{\mu}_c$  is called a critical point, and bifurcations may occur from  $\mathbf{x}_e(\boldsymbol{\mu})$ . To determine the stability of the equilibrium solution, we need to find the eigenvalues of the Jacobian  $\mathbf{J}(\boldsymbol{\mu})$ , which are the roots of the following characteristic polynomial equation:

$$\begin{aligned} P_n(L) &= \det[LI - \mathbf{J}(\boldsymbol{\mu})] \\ &= L^n + a_1(\boldsymbol{\mu})L^{n-1} + a_2(\boldsymbol{\mu})L^{n-2} \\ &\quad + \dots + a_{n-1}(\boldsymbol{\mu})L + a_n(\boldsymbol{\mu}) = 0. \end{aligned} \quad (3)$$

If for a value of  $\boldsymbol{\mu}$ , all the roots of the polynomial  $P_n(L)$  have negative real part, then the equilibrium solution is asymptotically stable for this value of  $\boldsymbol{\mu}$ . If at least one of the eigenvalues has zero real part as  $\boldsymbol{\mu}$  crosses a critical point  $\boldsymbol{\mu}_c$ , then the equilibrium solution becomes unstable at  $\boldsymbol{\mu}_c$  and bifurcation occurs from this critical point. When all the roots of  $P_n(L)$  have negative real part, we call  $P_n(L)$  a *stable polynomial*, otherwise an *unstable polynomial*.

In general, for  $n \geq 3$ , it is hard or impossible to find the roots of  $P_n(L)$ . Thus we use the Routh–Hurwitz criterion [Hinrichsen & Pritchard, 2005] to analyze the local stability of the equilibrium solution  $x = \mathbf{x}_e(\boldsymbol{\mu})$ . The criterion states that the necessary and sufficient conditions, under which the corresponding equilibrium is locally asymptotically stable, i.e. all the roots of the characteristic polynomial  $P_n(L)$  have negative real part, are given by

$$\Delta_i(\boldsymbol{\mu}) > 0, \quad i = 1, 2, \dots, n, \quad (4)$$

where  $\Delta_i(\boldsymbol{\mu})$  are called the  $i$ th-principal minors of the Hurwitz arrangements of order  $n$ , defined as follows (here, order  $n$  means that there are  $n$  coefficients  $a_i$  ( $i = 1, 2, \dots, n$ ) in Eq. (3), which construct the Hurwitz principal minors):

$$\begin{aligned} \Delta_1 &= a_1, \quad \Delta_2 = \det \begin{bmatrix} a_1 & 1 \\ a_3 & a_2 \end{bmatrix}, \\ \Delta_3 &= \det \begin{bmatrix} a_1 & 1 & 0 \\ a_3 & a_2 & a_1 \\ a_5 & a_4 & a_3 \end{bmatrix}, \quad \dots, \quad \Delta_n = a_n \Delta_{n-1}. \end{aligned} \quad (5)$$

Suppose as  $\boldsymbol{\mu}$  is varied to reach a critical point  $\boldsymbol{\mu} = \boldsymbol{\mu}_c$ , at least one of  $\Delta_i$ 's becomes zero, then the fixed point  $\mathbf{x}_e(\boldsymbol{\mu}_c)$  becomes unstable, and  $\boldsymbol{\mu}_c$  is called critical point. It is easy to see from Eq. (3) that if  $a_n(\boldsymbol{\mu}) = 0$  (then  $\Delta_n = 0$ ), but other Hurwitz arrangements are still positive (i.e.  $\Delta_i(\boldsymbol{\mu}) > 0$ ,  $i = 1, 2, \dots, (n-1)$ ),  $P_n(L) = 0$  has one zero root, indicating that system (2) has a simple zero singularity and a static bifurcation occurs from  $\mathbf{x}_e$ . For other complex dynamical behavior, for example, Hopf bifurcation occurs at a critical point at which  $P_n(L) = 0$  has a pair of purely imaginary eigenvalues,  $\pm i\omega$  ( $\omega > 0$ ). But this pair of purely imaginary eigenvalues are often difficult to be determined explicitly for high dimensional systems. Based on the Hurwitz criterion, the following theorem states the necessary and sufficient conditions for determining a Hopf critical point without computing the eigenvalues of the Jacobian of the corresponding system. Its proof can be found in [Yu, 2005].

**Theorem 1** [Yu, 2005]. *The necessary and sufficient conditions for system (2) to have a Hopf bifurcation at an equilibrium solution  $\mathbf{x} = \mathbf{x}_e$  is  $\Delta_{n-1} = 0$ , with other Hurwitz conditions being still held, i.e.  $a_n > 0$  and  $\Delta_i > 0$ , for  $i = 1, \dots, n-2$ .*

## 2.1. Equilibrium solutions

Having established the results for general nonlinear dynamical systems in the previous subsection, we now return to model (1). The equilibrium solutions of this model can be obtained by simply setting  $\dot{A} = \dot{R}_n = \dot{R}_a = \dot{E} = 0$  and solving the resulting algebraic equations, which yields two equilibrium solutions: the disease-free equilibrium  $E_0$  and the disease equilibrium  $E_1$ . They are given by

$$\begin{aligned} E_0 &: (0, 0, 0, 0) \\ E_1 &: \left( A_1, \bar{R}_n, \frac{c\xi \bar{R}_n}{\mu_d}, \right. \\ &\quad \left. \frac{[\sigma_1 \bar{R}_n(\mu_d + dc\xi) + \mu_d(b_1 + \mu_A)]A_1}{\mu_d \alpha} \right), \end{aligned}$$

Table 1. Parameter values used in model (1) [Alexander & Wahl, 2011].

Parameter	Value	Parameter	Value
$\pi_3$	0.0256 day <sup>-1</sup> per $E$ per $A$ ( $\pi_3$ )	$\beta$	200 day <sup>-1</sup> per $A$
$\lambda_E$	1000 day <sup>-1</sup> per $A$	$b_1$	0.25 day <sup>-1</sup> per $E$
$\sigma_{1,3}$	$3 \times 10^{-6}$ day <sup>-1</sup> per $R$ (or $R_n$ or $R_d$ ) per $A$	$b_3$	0.25 day <sup>-1</sup> per $E$
$\mu_A$	0.2 day <sup>-1</sup> per $A$	$\mu_E$	0.2 day <sup>-1</sup> per $E$
$\mu_n$	0.1 day <sup>-1</sup> per $R_n$	$\mu_d$	0.2 day <sup>-1</sup> per $R_d$
$\xi$	0.025 per $R_n$	$\alpha$	Bifurcation parameter
$d$	2	$c$	$2^3 = 8$

$$\bar{R}_n = \frac{\mu_d[\pi_3(b_1 + \mu_A)A_1 + \beta\alpha]A_1}{\mu_d\alpha(\mu_n + \xi) - \pi_3\sigma_1(\mu_d + dc\xi)A_1^2}, \tag{6}$$

where  $A_1$  is given in a function of the system parameters, particularly in  $\alpha$ , which is implicitly determined by the following fourth-degree polynomial equation in  $A_1$ :

$$F_1(A_1, \alpha) = \frac{81}{38146972656250}A_1^4 - \frac{1521}{625000000}\alpha A_1^2 - \frac{81}{10000000}\alpha A_1 + \frac{5}{8}\alpha^2 - \frac{81}{640000}\alpha = 0, \tag{7}$$

in which the parameter values given in Table 1 have been used. Note that the rational numbers given in this equation are obtained by using symbolic computation in which all the parameter values given in digital format (see Table 1) have been transformed to rational numbers for the convenience of computation.

The graph showing the component  $A$  of the equilibrium solutions  $E_0$  and  $E_1$ , i.e.  $A = 0$  and  $A = A_1$  satisfying  $F_1(A_1, \alpha) = 0$ , is given in Fig. 1. Note that a complete bifurcation diagram is depicted in Fig. 1(a), while its part which has biological meaning is given in Fig. 1(b). In order

to display the biologically meaningful solutions, a three-dimensional plot is shown in Fig. 1(c), indicating that one branch of each solution in Fig. 1(a) is biologically meaningless.

## 2.2. Stability of the equilibria

For the stability of the disease-free equilibrium  $E_0$ , the characteristic equation method and Lyapunov function method have been used in [Zhang *et al.*, 2014] to obtain the following result.

**Lemma 1.** *When  $\alpha < \alpha_t = \frac{1}{\lambda_E}(b_1 + \mu_A)(b_3 + \mu_E)\alpha_t$ , the disease-free equilibrium  $E_0$  of model (1) is globally asymptotically stable. It loses stability at  $\alpha = \alpha_t$  and becomes unstable for  $\alpha > \alpha_t$ .*

Next, consider the stability of the disease equilibrium  $E_1$ . Evaluating the Jacobian of (1) at  $E_1$  yields a fourth-degree characteristic polynomial, given by

$$P_1(L, A_1, \alpha) = L^4 + a_1(A_1, \alpha)L^3 + a_2(A_1, \alpha)L^2 + a_3(A_1, \alpha)L + a_4(A_1, \alpha) = 0 \tag{8}$$

where the coefficients  $a_1(A_1, \alpha)$ ,  $a_2(A_1, \alpha)$ ,  $a_3(A_1, \alpha)$ , and  $a_4(A_1, \alpha)$  are expressed in terms of  $A_1$  and  $\alpha$ , with other parameter values taken from Table 1, given below:

$$a_1(A_1, \alpha) = \frac{1}{40(18A_1^2 - 9765625\alpha)}(234A_1^2 - 11250000\alpha A_1 - 478515625\alpha),$$

$$a_2(A_1, \alpha) = \frac{1}{5000(18A_1^2 - 9765625\alpha)^2}[972A_1^5 + (1620000000\alpha + 20250)A_1^4 + 8226562500\alpha A_1^3 + (-1856689453125000\alpha^2 + 268066406250\alpha)A_1^2 - 10929107666015625\alpha^2 A_1 + 476837158203125000000\alpha^3 - 247955322265625000\alpha^2],$$

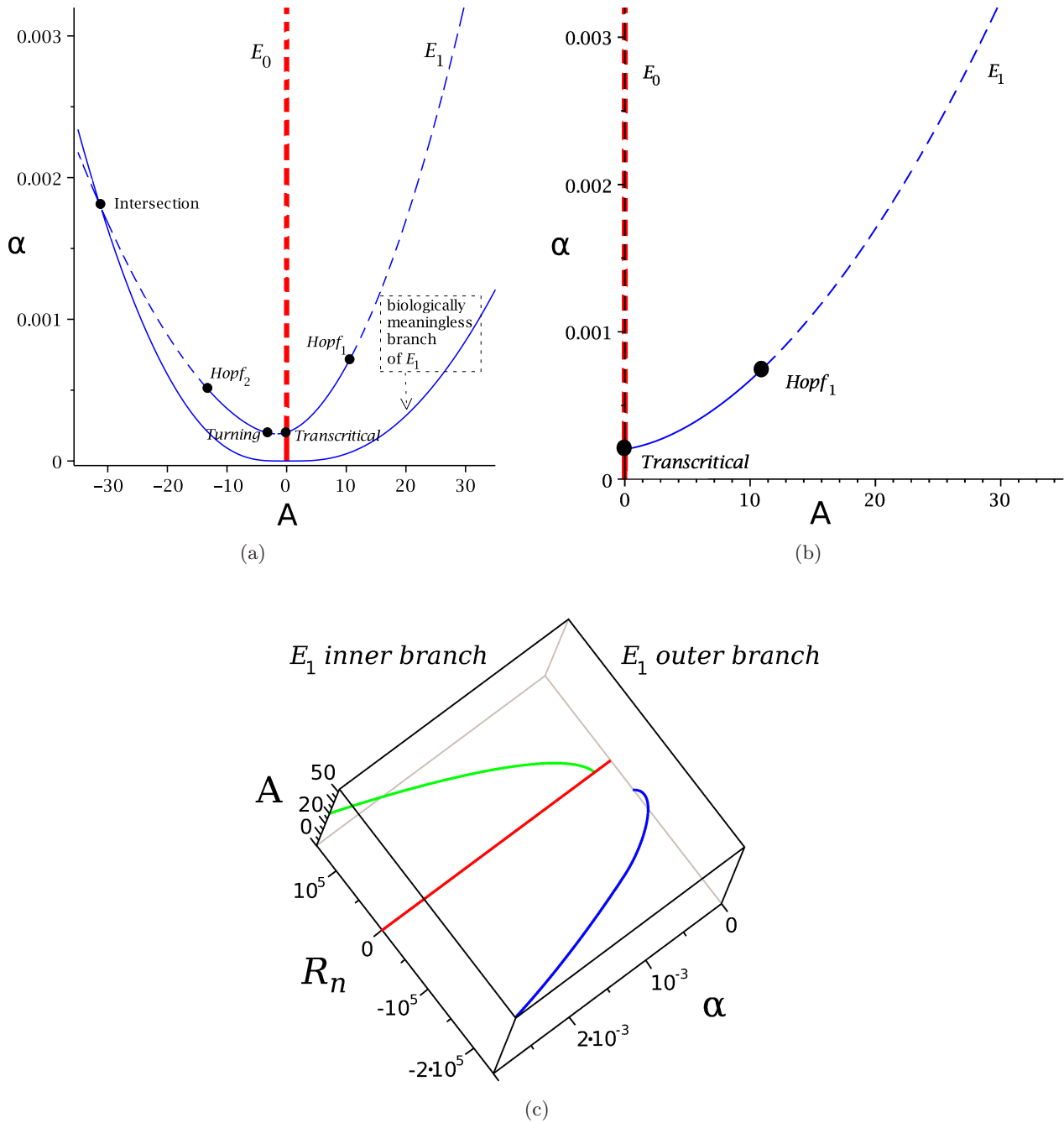


Fig. 1. (a) Complete bifurcation diagram for model (1) projected on the  $\alpha$ - $A$  plane, with the red and blue lines denoting  $E_0$  and  $E_1$ , respectively; (b) a part of bifurcation diagram in (a), restricted to the first quadrant and (c) bifurcation diagram for model (1) projected on the  $\alpha$ - $A$ - $R_n$  space, with the red, green and blue lines denoting  $E_0$ , the inner branch of  $E_1$ , and the outer branch of  $E_1$  which is biologically meaningless since  $R_n$  takes negative values. Here, the dotted and solid lines indicate unstable and stable equilibria, respectively.

$$\begin{aligned}
 a_3(A_1, \alpha) &= \frac{1}{10000000(18A_1^2 - 9765625\alpha)^2} [248832A_1^6 - 1166400A_1^5 - (1307812500000\alpha + 72900000)A_1^4 \\
 &\quad + 632812500000\alpha A_1^3 + (1296569824218750000\alpha + 44494628906250)\alpha A_1^2 \\
 &\quad + 5561828613281250000\alpha^2 A_1 - 309944152832031250000000\alpha^3 + 84221363067626953125\alpha^2], \\
 a_4(A_1, \alpha) &= \frac{1}{50000000(18A_1^2 - 9765625\alpha)^2} [746496A_1^6 - 1169437500000\alpha A_1^4 + 5695312500000\alpha A_1^3 \\
 &\quad + (733337402343750000\alpha + 133483886718750)\alpha A_1^2 + 3089904785156250000\alpha^2 A_1 \\
 &\quad - 119209289550781250000000\alpha^3 + 24139881134033203125\alpha^2].
 \end{aligned}$$

Based on the characteristic polynomial (8), we consider possible bifurcations from  $E_1$ , including both static bifurcation and dynamic (Hopf) bifurcations. First, the static bifurcation occurs when  $P_1(L, A_1, \alpha) = 0$  has zero roots (zero eigenvalues). The simplest case is single zero, i.e. when  $a_4(A_1, \alpha) = 0$ , and  $A_1$  should simultaneously satisfy  $F_1(A_1, \alpha) = 0$  [see Eq. (7)]. Thus, we obtain

$$A_{1s}(\alpha_s) = -\frac{21333593750000000\alpha_s^3 + 26617447265625\alpha_s^2 - 49464843750\alpha_s + 8748000}{3525388312500\alpha_s^2 - 4572342000\alpha_s + 979776}, \quad (9)$$

where  $\alpha_s$  is determined from the equation,

$$\begin{aligned}
 F_2(\alpha_s) &= \alpha_s(13530125\alpha_s - 2592)(400000\alpha_s - 81) \\
 &= 0.
 \end{aligned} \quad (10)$$

Solving  $F_2(\alpha_s) = 0$  for  $\alpha_s$ , and then substituting the solutions into  $A_{1s}(\alpha_s)$  using Eq. (9), yields three critical values. The first one defines a transcritical bifurcation point  $(\alpha_t, A_t) = (\frac{81}{400000}, 0) = (0.2025 \times 10^{-3}, 0)$ , which is exactly the same as that which we obtained from the disease-free equilibrium  $E_0$ ,  $\alpha_t = \frac{1}{\lambda_E}(b_1 + \mu_A)(b_3 + \mu_E) = \frac{1}{1000}(\frac{1}{4} + \frac{1}{5})^2 = \frac{81}{400000}$ . Here, the subscript “t” denotes transcritical bifurcation. Moreover, at this critical point, all other Hurwitz arrangements are still positive:  $\Delta_1 = \frac{49}{40}$ ,  $\Delta_2 = \frac{5863}{16000}$ , and  $\Delta_3 = \frac{52767}{6400000}$ . This implies that the two equilibrium solutions  $E_0$  and  $E_1$  actually intersect at this critical point, and the equilibrium  $E_1$  emerges. That is, the biologically meaningful equilibrium solution  $E_1$  exists only for  $\alpha \geq \alpha_t$  and no further static bifurcation can occur from  $E_1$  for  $\alpha > \alpha_t$ . The second critical value defines a turning point  $(\alpha_{\text{Turning}}, A_{\text{Turning}}) = (\frac{2592}{13530125}, -\frac{1125}{658})$ , which has a negative value for  $A$  and so is not biologically interesting [see Fig. 1(a)]. The third critical value is  $(\alpha_s, A_{1s}) = (0, 0)$ , which is not allowed since  $\alpha$  must take positive values for the components  $\bar{R}_n$  and  $\bar{E}$  in the equilibrium solution  $E_1$  [see Eq. (6)]. Therefore, the equation  $F_2(\alpha_s)$  defines a unique transcritical bifurcation point.

Next, we turn to consider possible Hopf bifurcations which may occur from the disease

equilibrium  $E_1$ . To achieve this, we apply Theorem 1 to the equilibrium  $E_1$ , where  $A_1$  satisfies the polynomial equation  $F_1(A_1, \alpha) = 0$  in (7). Based on the fourth-degree characteristic polynomial  $P_1(L, A_1, \alpha)$  [see Eq. (8)], we apply the formula,  $\Delta_3(A_1, \alpha) = a_1 a_2 a_3 - a_3^2 - a_1^2 a_4$  to solve the two polynomial equations,  $\Delta_3(A_1, \alpha) = 0$  and  $F_1(A_1, \alpha) = 0$ , together with the parameter values given in Table 1, yielding two Hopf bifurcation points:  $(\alpha_{H1}, A_{H1}) \approx (0.7867 \times 10^{-3}, 11.4436)$ , and  $(\alpha_{H2}, A_{H2}) \approx (0.5039 \times 10^{-3}, -13.1534)$ , as shown in Fig. 1(a). We only take the biologically meaningful point with two positive entries to get a unique Hopf bifurcation point:  $(\alpha_H, A_H) \approx (0.7867 \times 10^{-3}, 11.4436)$ . Here, the subscript “H” stands for Hopf bifurcation. At the critical point  $(\alpha_H, A_H)$ , other stability conditions given in Theorem 1 are still satisfied:

$$\begin{aligned}
 a_1 &\approx 2.098879937, & a_2 &\approx 0.6310564343, \\
 a_3 &\approx 0.1144843602, & a_4 &\approx 0.0314460534, \\
 \Delta_2 &\approx 1.2100273294, & \Delta_3 &\approx -0.1 \times 10^{-18} \approx 0.
 \end{aligned}$$

As a matter of fact, by using these given parameter values, we may numerically compute the Jacobian of system (1) at the equilibrium  $E_1$  to obtain a purely imaginary pair and two negative real eigenvalues:  $\pm 0.2335i, -1.7739$ , and  $-0.325$ . Therefore, the disease equilibrium  $E_1$  is stable for  $\alpha \in (\alpha_t, \alpha_H) \approx (0.2025 \times 10^{-3}, 0.7867 \times 10^{-3})$  and loses its stability

at  $\alpha = \alpha_H$ , where a Hopf bifurcation occurs, leading to bifurcation of a family of limit cycles.

In the next section, we will study the Hopf bifurcation from  $E_1$  and use center manifold theory and normal form theory to consider stability and direction of bifurcating limit cycles.

### 3. Hopf Bifurcation and Limit Cycles: Nonlinear Analysis

In this section, we pay attention to the Hopf bifurcation determined in the previous section, and use center manifold theory and normal form theory to find the approximate solutions of the limit cycles and determine their stability. In the following, for convenience, we first briefly describe center manifold theory and normal form theory. Suppose a dynamical system under consideration is described by the following differential equation (D.E.),

$$\begin{aligned} \dot{\bar{\mathbf{x}}} &= \mathbf{F}(\bar{\mathbf{x}}, \bar{\boldsymbol{\mu}}), \quad \bar{\mathbf{x}} \in \mathbf{R}^n, \quad \bar{\boldsymbol{\mu}} \in \mathbf{R}^k, \\ \mathbf{F} &: \mathbf{R}^{n+k} \rightarrow \mathbf{R}^n, \end{aligned} \quad (11)$$

where  $\bar{\mathbf{x}} = (\bar{x}_1, \bar{x}_2, \dots, \bar{x}_n)$  is a state vector,  $\bar{\boldsymbol{\mu}} = (\bar{\mu}_1, \bar{\mu}_2, \dots, \bar{\mu}_n)$  is a parameter vector, and the nonlinear vector function  $\mathbf{F}$  is assumed to be analytic in  $\bar{\mathbf{x}}$  and  $\bar{\boldsymbol{\mu}}$ . The equilibrium solution  $\bar{\mathbf{x}}_e = \bar{\mathbf{x}}_e(\bar{\boldsymbol{\mu}})$  of (11) is determined from  $\mathbf{F}(\bar{\mathbf{x}}, \bar{\boldsymbol{\mu}}) = 0$ . We consider Hopf bifurcation, so set  $k = 1$  and assume the Jacobian of the system evaluated at the equilibrium solution  $\bar{\mathbf{x}}_e$  is given by  $J(\mu) = D_{\bar{\mathbf{x}}}\mathbf{F}(\bar{\mathbf{x}}_e, \bar{\boldsymbol{\mu}})$ , which has a pair of purely imaginary eigenvalues at a critical point  $\bar{\boldsymbol{\mu}} = \bar{\boldsymbol{\mu}}_c$ , and other eigenvalues have negative real part.

Now, we first apply center manifold theory to reduce the dimension of system (11) and obtain a simplified differential system on the center manifold. Then we apply normal form theory to further simplify the resulting differential system, and perform a bifurcation study of a given type. To achieve this, we introduce a sliding transformation  $\bar{\mathbf{x}} = \bar{\mathbf{x}}_e(\bar{\boldsymbol{\mu}}) + \mathbf{u}$ , and a parameter shifting  $\bar{\boldsymbol{\mu}} = \bar{\boldsymbol{\mu}}_c + \mu$  into system (11) to obtain

$$\begin{aligned} \dot{\mathbf{u}} &= \mathbf{F}(\bar{\mathbf{x}}_e(\bar{\boldsymbol{\mu}}_c + \mu) + \mathbf{u}, \bar{\boldsymbol{\mu}}_c + \mu) \\ &= \tilde{\mathbf{F}}(\mathbf{u}, \mu), \end{aligned}$$

which yields  $D_{\mathbf{u}}\tilde{\mathbf{F}}(\mathbf{0}, 0) = \tilde{J}$  whose eigenvalues contain an imaginary pair. In addition, introducing another linear transformation  $\mathbf{u} = T\mathbf{x}$  such that  $J = T^{-1}\tilde{J}T$  is in Jordan canonical form, therefore, we obtain the following general D.E.:

$$\dot{\mathbf{x}} = \mathbf{f}(\mathbf{x}, \mu), \quad \mathbf{x} \in \mathbf{R}^n, \quad \mu \in \mathbf{R}, \quad \mathbf{f} : \mathbf{R}^{n+1} \rightarrow \mathbf{R}^n, \quad (12)$$

where  $\mathbf{f}(\mathbf{x}, \mu) = T^{-1}\tilde{\mathbf{F}}(T\mathbf{x}, \mu)$ . Now  $\mathbf{x} = \mathbf{0}$  is an equilibrium solution of system (12) for any real values of  $\mu$ , i.e.

$$\mathbf{f}(\mathbf{0}, \mu) \equiv \mathbf{0} \quad \text{and}$$

$$J(\mu) = D_{\mathbf{x}}\mathbf{f}(\mathbf{0}, \mu) = \begin{bmatrix} A(\mu) & 0 \\ 0 & B(\mu) \end{bmatrix}$$

with

$$J(0) = \begin{bmatrix} A(0) & 0 \\ 0 & B(0) \end{bmatrix}$$

satisfying

$$\text{Re}(\lambda(A(0))) = 0, \quad \text{Re}(\lambda(B(0))) < 0.$$

$\lambda(\cdot)$  stands for the eigenvalues of a given matrix. Then, we can rewrite (12) as

$$\begin{aligned} \dot{\mathbf{x}}_c &= A(\mu)\mathbf{x}_c + \mathbf{f}_c(\mathbf{x}_c, \mathbf{x}_s; \mu), \\ \dot{\mathbf{x}}_s &= B(\mu)\mathbf{x}_s + \mathbf{f}_s(\mathbf{x}_c, \mathbf{x}_s; \mu), \end{aligned} \quad (13)$$

where  $\mathbf{x} = (\mathbf{x}_c, \mathbf{x}_s)^T$ ,  $\mathbf{x}_c$  and  $\mathbf{x}_s$  are state variables associated with the eigenvalues of the linearized systems with zero and negative real parts, respectively.  $n_c + n_s = n$  (for Hopf bifurcation,  $n_c = 2$ ), and

$$A(\mu) = A + \bar{A}\mu, \quad B(\mu) = B + \bar{B}\mu. \quad (14)$$

Moreover,  $\mathbf{f}_c$  and  $\mathbf{f}_s$  satisfy  $\mathbf{f}_c(\mathbf{0}, \mathbf{0}; 0) = \mathbf{f}_s(\mathbf{0}, \mathbf{0}; 0) = 0$  and  $\frac{\partial \mathbf{f}_c(\mathbf{0}, \mathbf{0}; 0)}{\partial \mathbf{x}_c} = \frac{\partial \mathbf{f}_c(\mathbf{0}, \mathbf{0}; 0)}{\partial \mathbf{x}_s} = \frac{\partial \mathbf{f}_c(\mathbf{0}, \mathbf{0}; 0)}{\partial \mu} = \frac{\partial \mathbf{f}_s(\mathbf{0}, \mathbf{0}; 0)}{\partial \mathbf{x}_c} = \frac{\partial \mathbf{f}_s(\mathbf{0}, \mathbf{0}; 0)}{\partial \mathbf{x}_s} = \frac{\partial \mathbf{f}_s(\mathbf{0}, \mathbf{0}; 0)}{\partial \mu} = 0$ . By center manifold theory, there exists an analytic function  $\mathbf{h}$ , such that  $\mathbf{x}_s = \mathbf{h}(\mathbf{x}_c; \mu)$  with  $\mathbf{h}(\mathbf{0}; 0) = D\mathbf{h}(\mathbf{0}; 0) = \mathbf{0}$ . Thus,  $\dot{\mathbf{x}}_s = D\mathbf{h}(\mathbf{x}_c; \mu)\dot{\mathbf{x}}_c$ , which can be rewritten as

$$\begin{aligned} \mathcal{N}(\mathbf{h}(\mathbf{x}_c; \mu)) &\equiv D\mathbf{h}(\mathbf{x}_c; \mu)[A(\mu)\mathbf{x}_c + \mathbf{f}_c(\mathbf{x}_c, \mathbf{h}(\mathbf{x}_c; \mu); \mu)] \\ &\quad - B(\mu)\mathbf{h}(\mathbf{x}_c; \mu) - \mathbf{f}_s(\mathbf{x}_c, \mathbf{h}(\mathbf{x}_c; \mu); \mu) = 0. \end{aligned} \quad (15)$$

In general, the above equation with the boundary conditions  $\mathbf{h}(\mathbf{0}; 0) = D\mathbf{h}(\mathbf{0}; 0) = \mathbf{0}$  cannot be solved analytically. To find the approximation of  $\mathbf{h}(\mathbf{x}_c; \mu)$ , we use the Taylor series of  $\mathbf{h}(\mathbf{x}_c; \mu)$  expanded near  $(\mathbf{x}_c; \mu) = (\mathbf{0}; 0)$  with undetermined coefficients, and then expanding (15) and balancing the coefficients of like powers to determine the coefficients in  $\mathbf{h}(\mathbf{x}_c; \mu)$ , and so an approximation of  $\mathbf{x}_s = \mathbf{h}(\mathbf{x}_c; \mu)$  is obtained.

We now consider the projection of the vector field on the center manifold  $W^c = \{(\mathbf{x}_c, \mathbf{x}_s) \mid \mathbf{x}_s = \mathbf{h}(\mathbf{x}_c; \mu)\}$ , yielding  $\dot{\mathbf{x}}_c = A(\mu)\mathbf{x}_c + \mathbf{f}_c(\mathbf{x}_c, \mathbf{h}(\mathbf{x}_c; \mu); \mu)$  or

$$\dot{\mathbf{x}}_c = A(\mu)\mathbf{x}_c + \mathbf{f}_c(\mathbf{x}_c; \mu), \quad \mathbf{x}_c \in \mathbf{R}^2, \quad \mu \in \mathbf{R}, \quad (16)$$

satisfying  $\mathbf{f}_c(\mathbf{0}; 0) = D\mathbf{f}_c(\mathbf{0}; 0) = 0$ , and  $A(\mu) = A + \bar{A}\mu$  where  $A = \begin{bmatrix} 0 & \omega \\ -\omega & 0 \end{bmatrix}$  and  $\bar{A} = \begin{bmatrix} a_{11} & a_{12} \\ a_{21} & a_{22} \end{bmatrix}$ . Now applying the method of normal forms to system (16) and putting the result in the polar coordinates, yields

$$\begin{aligned} \dot{r} &= r(v_0\mu + v_1r^2 + v_2r^4 + \dots), \\ \dot{\theta} &= \omega + \tau_0\mu + \tau_1r^2 + \tau_2r^4 + \dots, \end{aligned} \quad (17)$$

where  $r$  and  $\theta$  denote the amplitude and phase of motion, respectively;  $v_0$  and  $\tau_0$  can be obtained

from linear analysis, while  $v_1, v_2, \dots$  and  $\tau_1, \tau_2, \dots$  are obtained from nonlinear analysis. We have the following theorem for finding  $v_0$  and  $\tau_0$ .

**Theorem 2.** For the linearized system of (16),

$$\dot{\mathbf{x}}_c = A(\mu)\mathbf{x}_c = \begin{bmatrix} a_{11}\mu & \omega + a_{12}\mu \\ -\omega + a_{21}\mu & a_{22}\mu \end{bmatrix} \mathbf{x}_c,$$

the following holds:

$$\begin{aligned} v_0 &= \frac{1}{2}(a_{11} + a_{22}), \\ \tau_0 &= \frac{1}{2}(a_{12} - a_{21}). \end{aligned} \quad (18)$$

*Proof.* This is a two-dimensional system. Let  $\mathbf{x}_c = (x_{c1}, x_{c2})^T$ . There exists a nonsingular matrix  $P$ , given by

$$P = \begin{bmatrix} -(\omega + a_{12}\mu) & 0 \\ \frac{1}{2}(a_{11} - a_{22})\mu & -\sqrt{\omega^2 + \omega(a_{12} - a_{21})\mu + \left[a_{12}a_{21} - \frac{1}{4}(a_{11} - a_{22})^2\right]\mu^2} \end{bmatrix}, \quad (19)$$

which is used in the transformation  $(x_{c1}, x_{c2})^T = P(y_1, y_2)^T$  to yield

$$\begin{pmatrix} \dot{y}_1 \\ \dot{y}_2 \end{pmatrix} = P^{-1}AP \begin{pmatrix} y_1 \\ y_2 \end{pmatrix} = \begin{bmatrix} \frac{1}{2}(a_{11} + a_{22})\mu & \bar{\omega} \\ -\bar{\omega} & \frac{1}{2}(a_{11} + a_{22})\mu \end{bmatrix} \begin{pmatrix} y_1 \\ y_2 \end{pmatrix}, \quad (20)$$

where  $P^{-1}$  is the inverse matrix of  $P$ , and

$$\bar{\omega} = \omega \sqrt{1 + \frac{1}{\omega}(a_{12} - a_{21})\mu + \frac{1}{\omega^2} \left[ a_{12}a_{21} - \frac{1}{4}(a_{11} - a_{22})^2 \right] \mu^2}.$$

Next, we put the new system (20) in polar coordinates, via  $y_1 = r \sin \theta$ ,  $y_2 = r \cos \theta$ . Thus,  $r^2 = y_1^2 + y_2^2$ , and  $\tan \theta = \frac{y_1}{y_2}$ . Therefore,  $2r\dot{r} = 2y_1\dot{y}_1 + 2y_2\dot{y}_2$ , yielding

$$\dot{r} = \frac{1}{2}(a_{11} + a_{22})\mu r = v_0\mu r \quad (21)$$

and  $\dot{\theta} \sec^2 \theta = \frac{\dot{x}_1 x_2 - \dot{x}_2 x_1}{x_2^2}$ , gives

$$\begin{aligned} \dot{\theta} &= \frac{\dot{x}_1 x_2 - \dot{x}_2 x_1}{\left(1 + \frac{x_1^2}{x_2^2}\right) x_2^2} = \omega \sqrt{1 + \frac{1}{\omega}(a_{12} - a_{21})\mu + \frac{1}{\omega^2} \left[ a_{12}a_{21} - \frac{1}{4}(a_{11} - a_{22})^2 \right] \mu^2} \\ &= \omega \left[ 1 + \frac{1}{2\omega}(a_{12} - a_{21})\mu \right] + O(\mu^2) = \omega + \frac{1}{2}(a_{12} - a_{21})\mu + O(\mu^2) = \omega + \tau_0\mu + O(\mu^2). \end{aligned} \quad (22)$$

The proof of Theorem 2 is complete. ■

Note that if the original system is a nonlinear system, given in the general form,  $\dot{\mathbf{x}}_c = \mathbf{f}(\mathbf{x}_c, \mu)$ , with  $\mathbf{f}(\mathbf{0}, 0) = 0$ , and  $J(\mathbf{0}, 0) = D_{\mathbf{x}_c} \mathbf{f}(\mathbf{0}, 0) = \begin{bmatrix} 0 & \omega \\ -\omega & 0 \end{bmatrix}$ , then  $a_{ij} = \frac{\partial f_i^2}{\partial x_j \partial \mu}$ ,  $i, j = 1, 2$ .

Finally, to find  $v_1, v_2, \dots$  and  $\tau_1, \tau_2, \dots$ , we set  $\mu = \mu_c = 0$  in system (16) to consider

$$\begin{aligned} \dot{\mathbf{x}}_c &= A(0)\mathbf{x}_c + \mathbf{f}_c(\mathbf{x}_c, \mathbf{h}(\mathbf{x}_c; 0); 0) \\ &= A\mathbf{x}_c + \mathbf{f}_c(\mathbf{x}_c) \end{aligned}$$

and apply normal form theory (e.g. see [Guckenheimer & Holmes, 1990]) to obtain

$$\begin{aligned} \dot{x}_{c1} &= x_{c1}[v_1(x_{c1}^2 + x_{c2}^2) + v_2(x_{c1}^2 + x_{c2}^2)^2 + \dots] \\ &\quad + x_{c2}[\omega + \tau_1(x_{c1}^2 + x_{c2}^2) + \tau_2(x_{c1}^2 + x_{c2}^2)^2 + \dots], \\ \dot{x}_{c2} &= -x_{c1}[\omega + \tau_1(x_{c1}^2 + x_{c2}^2) + \tau_2(x_{c1}^2 + x_{c2}^2)^2 + \dots] \\ &\quad + x_{c2}[v_1(x_{c1}^2 + x_{c2}^2) + v_2(x_{c1}^2 + x_{c2}^2)^2 + \dots], \end{aligned}$$

which can be written via  $x_{c1} = r \sin \theta$ ,  $x_{c2} = r \cos \theta$  as

$$P = \begin{bmatrix} -0.0001169099 & -0.0002184341 & -0.0008788039 & -0.0001219983 \\ -0.8049052552 & 0.0 & 0.1059811404 & 0.5249612314 \\ -0.3405368387 & 0.3976613541 & -0.0134675000 & -0.8399379702 \\ -0.1318126011 & -0.2462783299 & 0.9942765471 & -0.1375496158 \end{bmatrix}$$

we introduce the affine transformation,

$$\begin{pmatrix} A \\ R_n \\ R_d \\ E \end{pmatrix} = \begin{pmatrix} \bar{A}(\mu) \\ \bar{R}_n(\bar{A}(\mu), \mu) \\ \bar{R}_d(\bar{A}(\mu), \mu) \\ \bar{E}(\bar{A}(\mu), \mu) \end{pmatrix} + P \begin{pmatrix} x_1 \\ x_2 \\ x_3 \\ x_4 \end{pmatrix}, \tag{23}$$

where

$$\begin{aligned} \bar{R}_n(\bar{A}(\mu), \mu) &= \frac{-0.002304(\bar{A} + 13.65733522 + 17361.11111\mu)\bar{A}}{0.4608 \times 10^{-7}\bar{A}^2 - 0.1966656271 \times 10^{-4} - 0.025\mu}, \\ \bar{R}_d(\bar{A}(\mu), \mu) &= \frac{-0.002304(\bar{A} + 13.65733522 + 17361.11111\mu)\bar{A}}{0.4608 \times 10^{-7}\bar{A}^2 - 0.1966656271 \times 10^{-4} - 0.025\mu}, \\ \bar{E}(\bar{A}(\mu), \mu) &= \frac{-7812.5(0.02458320339 + 0.7866625085 \times 10^{-3}\bar{A} + \bar{A}\mu + 31.25\mu)\bar{A}}{(0.0007866625084 + \mu)(\bar{A}^2 - 426.7917255 - 542534.7222\mu)}, \end{aligned}$$

while  $\bar{A}$  and  $\mu$  have the following relation:

$$\begin{aligned} F_{4a} &= 0.21233664 \times 10^{-11}\bar{A}^4 + (-0.191442188 \times 10^{-8} - 0.24336 \times 10^{-5}\mu)\bar{A}^2 \\ &\quad - (0.6371966318 \times 10^{-8} + 0.81 \times 10^{-5}\mu)\bar{A} - 0.9956197372 \times 10^{-7} \\ &\quad - 0.1265625 \times 10^{-3}\mu + 0.625(0.7866625084 \times 10^{-3} + \mu)^2 = 0, \end{aligned}$$

$$\dot{r} = r(v_1 r^2 + v_2 r^4 + \dots),$$

$$\dot{\theta} = \omega + \tau_1 r^2 + \tau_2 r^4 + \dots$$

The proof can be found in [Yu, 1998].

It should be pointed out that the above two steps in computing the center manifold and normal form of general nonlinear systems can be combined into one procedure, e.g. see [Yu, 1998, 2003].

### 3.1. Normal form computation associated with the Hopf bifurcation from $E_1$

Now we apply normal form theory and the Maple program developed in [Yu, 1998] to system (1) to analyze the Hopf bifurcation which occurs at the critical point  $(\alpha_H, A_H) \approx (7.8666 \times 10^{-4}, 11.4436)$  (with other parameter values given in Table 1). We show the details of finding the normal form for system (1) associated with this Hopf critical point.

Let  $\alpha = \alpha_H + \mu$ , where  $\mu$  is a small perturbation (bifurcation) parameter. Then, with

into system (1) to obtain

$$\dot{x}_i = F_i(x_1, x_2, x_3, x_4; \mu), \quad i = 1, 2, 3, 4, \tag{24}$$

in which

$$\begin{aligned} F_1 = & 0.2335496834x_2 + 0.1 \times 10^{-5} \\ & + (79.07737301x_1 + 65.85310456x_2 - 917.0159663x_3 + 73.44534378x_4)\mu + o(\mu) \\ & + 0.6907346099 \times 10^{-7}x_1^2 - 0.7871759754 \times 10^{-6}x_1x_2 + 0.3970174728 \times 10^{-6}x_1x_3 \\ & + 0.283435609 \times 10^{-7}x_1x_4 - 0.2450834082 \times 10^{-6}x_3x_2 + 0.2071989330 \times 10^{-4}x_3^2 \\ & + 0.3049539696 \times 10^{-6}x_3x_4 - 0.1037827494 \times 10^{-5}x_4x_2 - 0.456398326 \times 10^{-7}x_4^2 \\ & - 0.1711886771 \times 10^{-5}x_2^2, \end{aligned}$$

$$\begin{aligned} F_2 = & -0.2335496834x_1 + 0.3 \times 10^{-5} \\ & + (600.2222024x_1 + 735.9644840x_2 - 1588.592053x_3 + 583.6348214x_4)\mu + o(\mu) \\ & + 0.1870133257 \times 10^{-5}x_1^2 + 0.2707944533 \times 10^{-5}x_1x_2 - 0.165759520 \times 10^{-6}x_1x_3 \\ & + 0.3428802216 \times 10^{-5}x_1x_4 - 0.1445942971 \times 10^{-6}x_3x_2 - 0.5061600581 \times 10^{-5}x_3^2 \\ & - 0.154680119 \times 10^{-6}x_3x_4 + 0.1939706942 \times 10^{-5}x_4x_2 + 0.1541570112 \times 10^{-5}x_4^2 \\ & - 0.1468948484 \times 10^{-5}x_2^2, \end{aligned}$$

$$\begin{aligned} F_3 = & -1.773879937x_3 - 0.2 \times 10^{-5} \\ & + (21.72751810x_1 + 168.3180208x_2 - 62.7868030x_3 + 36.82458413x_4)\mu + o(\mu) \\ & + 0.3 \times 10^{-15}x_1^2 - 0.5 \times 10^{-16}x_1x_2 + 0.4457936798 \times 10^{-5}x_1x_3 \\ & + 0.4 \times 10^{-15}x_1x_4 - 0.2385968125 \times 10^{-5}x_3x_2 - 0.2371384210 \times 10^{-6}x_3^2 \\ & + 0.3464744128 \times 10^{-5}x_3x_4 - 0.1 \times 10^{-15}x_4x_2 + 0.2 \times 10^{-15}x_4^2, \end{aligned}$$

$$\begin{aligned} F_4 = & -0.3250000000x_4 + 0.1 \times 10^{-5} \\ & + (251.7612101x_1 + 319.0383240x_2 - 379.3117812x_3 + 245.9493920x_4)\mu + o(\mu) \\ & + 0.8573938681 \times 10^{-6}x_1^2 + 0.1601198369 \times 10^{-5}x_1x_2 - 0.310918787 \times 10^{-6}x_1x_3 \\ & + 0.1611845343 \times 10^{-5}x_1x_4 + 0.6916390751 \times 10^{-7}x_3x_2 - 0.1079305444 \times 10^{-4}x_3^2 \\ & - 0.2524231766 \times 10^{-6}x_3x_4 + 0.1339104819 \times 10^{-5}x_4x_2 + 0.7483468117 \times 10^{-6}x_4^2 \\ & - 0.14090733 \times 10^{-8}x_2^2, \end{aligned}$$

where  $o(\mu)$  represents higher-order terms of  $\mu$ . Now, the Jacobian of system (24) evaluated on the equilibrium,  $x_i = 0, i = 1, 2, 3, 4$ , at the critical point,  $\mu = 0$  [corresponding to the disease equilibrium  $E_1$  for model (1)] is in the Jordan canonical form:

$$J = \begin{bmatrix} 0 & 0.233549683 & 0 & 0 \\ -0.233549683 & 0 & 0 & 0 \\ 0 & 0 & -1.773879938 & 0 \\ 0 & 0 & 0 & -0.3250000000 \end{bmatrix}.$$

Applying the formula (18) to system (24), we obtain

$$\begin{aligned} v_0 &= \frac{1}{2} \left( \frac{\partial^2 F_1}{\partial x_1 \partial \mu} + \frac{\partial^2 F_2}{\partial x_2 \partial \mu} \right) \Big|_{x_i=0, \mu=0} \\ &= 34.2047656142, \\ \tau_0 &= \frac{1}{2} \left( \frac{\partial^2 F_1}{\partial x_2 \partial \mu} - \frac{\partial^2 F_2}{\partial x_1 \partial \mu} \right) \Big|_{x_i=0, \mu=0} \\ &= 132.8997934535. \end{aligned} \quad (25)$$

Next, substituting  $\mu = 0$  into (24) and then applying the Maple program [Yu, 1998] yields

$$\begin{aligned} v_1 &= -0.2016072570 \times 10^{-11}, \\ \tau_1 &= -0.1318624299 \times 10^{-10}. \end{aligned} \quad (26)$$

Therefore, the normal form associated with this Hopf bifurcation, up to third-order terms, is given by

$$\begin{aligned} \dot{r} &= r(v_0\mu + v_1r^2) \\ &= r(34.2047656142\mu - 0.2016072570 \times 10^{-11}r^2), \\ \dot{\theta} &= \omega_c + \tau_0\mu + \tau_1r^2 \\ &= 0.233549683 + 132.8997934535\mu \\ &\quad - 0.1318624299 \times 10^{-10}r^2. \end{aligned} \quad (27)$$

The steady-state solutions of Eq. (27) are determined by  $\dot{r} = \dot{\theta} = 0$ , resulting in

$$\bar{r} = 0, \quad \bar{r}^2 \approx 0.1696603893 \times 10^{14}\mu. \quad (28)$$

The equilibrium  $\bar{r} = 0$  represents the disease equilibrium  $E_1$  of model (1). A linear analysis on the first differential equation of (27) shows that  $\frac{d}{dr}(\frac{dr}{dt})|_{\bar{r}=0} = v_0\mu$ , and thus  $\bar{r} = 0$  ( $E_1$ ) is stable (unstable) for  $\mu < 0$  ( $> 0$ ), as expected. When  $\mu$  is increased from negative to cross zero, a Hopf bifurcation occurs and the amplitude of the bifurcating limit cycles is approximated by the nonzero steady state solution,

$$\bar{r} \approx 0.4118985182 \times 10^7 \sqrt{\mu} \quad (\mu > 0). \quad (29)$$

Since  $\frac{d}{dr}(\frac{dr}{dt})|_{(29)} = 2v_1\bar{r}^2 = -2v_0\mu < 0$  ( $\mu > 0, v_0 > 0, v_1 < 0$ ), it indicates that the Hopf bifurcation is supercritical since  $v_1 < 0$  and so the bifurcating limit cycles are stable. Equation (29) gives the approximate amplitude of the bifurcating limit cycles, while the phase of the motion is determined by  $\theta = \omega t$ , where  $\omega$  is given by

$$\omega = \frac{d\theta}{dt} \Big|_{(29)} = 0.233549683 - 90.8185182\mu. \quad (30)$$

Having found the nonzero steady-state solution (limit cycle) in terms of  $\bar{r}$  and  $\theta = \omega t$ , the periodic solution of Eq. (24) can be written in a general form:

$$\begin{aligned} x_1(\mu) &= \bar{r} \cos(\omega t) + h_1(\bar{r} \cos(\omega t), \bar{r} \sin(\omega t)), \\ x_2(\mu) &= -\bar{r} \sin(\omega t) + h_2(\bar{r} \cos(\omega t), \bar{r} \sin(\omega t)), \\ x_i(\mu) &= h_i(\bar{r} \cos(\omega t), \bar{r} \sin(\omega t)), \quad i = 3, 4, \\ & \quad h_i \text{ starts from second-order term,} \end{aligned} \quad (31)$$

while the first-order approximation of the limit cycles is given by

$$\begin{aligned} x_1(\mu) &= \bar{r} \cos(\omega t), \\ x_2(\mu) &= -\bar{r} \sin(\omega t), \quad x_3 = x_4 = 0, \end{aligned}$$

where  $\bar{r}$  and  $\omega$  are given in Eqs. (29) and (30), respectively. However, in order to get higher-order (e.g. third-order) approximate solutions of the oscillation in terms of the original variables  $A$ ,  $R_n$ ,  $R_d$ , and  $E$  for a comparison with the numerical simulation to be discussed in the next section, we need the nonlinear transformations (including the center manifold transformation and the normal form transformation) between  $x_i$  ( $i = 1, 2, 3, 4$ ), and the polar coordinates  $(r, \theta)$ . Fortunately, these nonlinear transformations can be obtained directly from the computer output of the Maple program [Yu, 1998] as follows:

$$\begin{aligned} x_1(t) &= \cos(\omega t)\bar{r} + [0.8588852860 \times 10^{-6} - 0.3506344360 \times 10^{-5} \cos(2\omega t) \\ &\quad + 0.4474326340 \times 10^{-5} \sin(2\omega t)]\bar{r}^2 + [0.1097332343 \times 10^{-10} \cos(3\omega t) \\ &\quad + 0.3484198508 \times 10^{-10} \sin(3\omega t)]\bar{r}^3, \\ x_2(t) &= -\sin(\omega t)\bar{r} + [0.3517053177 \times 10^{-5} + 0.5135844613 \times 10^{-5} \cos(2\omega t) \\ &\quad + 0.5327445638 \times 10^{-5} \sin(2\omega t)]\bar{r}^2 - [0.3403071221 \times 10^{-10} \cos(\omega t) \end{aligned}$$

$$\begin{aligned}
 & + 0.4194098549 \times 10^{-11} \sin(\omega t) + 0.4874935933 \times 10^{-10} \cos(3\omega t) \\
 & - 0.532632423 \times 10^{-11} \sin(3\omega t)]\bar{r}^3, \\
 x_3(t) & = [0.8456040162 \times 10^{-16} + 0.7213644930 \times 10^{-16} \cos(2\omega t) + 0.4718182329 \times 10^{-16} \sin(2\omega t)]\bar{r}^2, \\
 x_4(t) & = [0.1316899684 \times 10^{-5} - 0.1841270059 \times 10^{-6} \sin(2\omega t) + 0.1585867935 \times 10^{-5} \cos(2\omega t)]\bar{r}^2 \\
 & + [0.1207672844 \times 10^{-10} \cos(\omega t) + 0.1812966212 \times 10^{-10} \sin(\omega t) \\
 & - 0.8220638067 \times 10^{-11} \cos(3\omega t) + 0.1214100228 \times 10^{-10} \sin(3\omega t)]\bar{r}^3.
 \end{aligned} \tag{32}$$

Finally, with the above transformations we can now use the affine transformation (23) to obtain the periodic solution in terms of the original variables. The comparison between the analytical prediction and numerical simulation is given in Sec. 5.

#### 4. Generalized Hopf Bifurcation Leading to Multiple Limit Cycles

In the previous sections, we have given a detailed analysis on Hopf bifurcation, which is limited to the bifurcation of single limit cycle. However, disease models may exhibit complex dynamical behaviors caused by bifurcation of multiple limit cycles, yielding bistable or multiple stable solutions involving equilibria and steady motions. It has been noted that such a study is often ignored in the literature on the analysis of practical systems, in particular, on biological systems, since the analysis is not easy even for two-dimensional systems. Most of the published works are limited to bifurcation of single limit cycle with very few of them using numerical simulation to show two limit cycles.

In this section, we will use the reduced three-dimensional model presented in [Zhang *et al.*, 2014] to prove the existence of two limit cycles bifurcating from a Hopf critical point. To reduce the four-dimensional system (1) to a three-dimensional model, we assume the following:

- (i) Only the suppression for which Treg ( $R_n$  and  $R_d$ ) acts on pAPC ( $A$ ), not on effector T cells ( $E$ ), is considered, resulting in  $\sigma_3 = 0$ .
- (ii) Except for  $E$ , the IL-2 sources are not considered, yielding  $\beta = 0$ .
- (iii) Quasi-steady state assumption is applied to the last equation of model (1), leading to  $\dot{E} \approx 0$ , and thus the state variable  $E$  can be eliminated from the system.

Under the above assumptions, system (1) becomes

$$\begin{aligned}
 \dot{A} & = \frac{\alpha\lambda_E}{b_3 + \mu_E} A - \sigma_1(R_n + dR_d)A \\
 & - (b_1 + \mu_A)A, \\
 \dot{R}_n & = \frac{\pi_3\lambda_E}{b_3 + \mu_E} A^2 - (\mu_n + \xi)R_n, \\
 \dot{R}_d & = c\xi R_n - \mu_d R_d.
 \end{aligned} \tag{33}$$

To further simplify the analysis, introducing the following transformation,

$$A = \mu_1 X, \quad R_n = \mu_2 Y, \quad R_d = \mu_3 Z, \quad \tau = \mu_4 t, \tag{34}$$

where

$$\begin{aligned}
 \mu_1 & = \mu_d \sqrt{\frac{b_3 + \mu_E}{\sigma_1 \pi_3 \lambda_E}}, \quad \mu_2 = \frac{\mu_d}{\sigma_1}, \\
 \mu_3 & = \frac{c\xi}{\sigma_1}, \quad \mu_4 = \mu_d,
 \end{aligned}$$

into (33) we obtain the dimensionless system:

$$\begin{aligned}
 \frac{dX}{d\tau} & = (m_1 - m_2 - Y - DZ)X, \\
 \frac{dY}{d\tau} & = X^2 - m_3 Y, \\
 \frac{dZ}{d\tau} & = Y - Z,
 \end{aligned} \tag{35}$$

where the new parameters are given by

$$\begin{aligned}
 m_1 & = \frac{\alpha\lambda_E}{\mu_d(b_3 + \mu_E)}, \quad m_2 = \frac{b_1 + \mu_A}{\mu_d}, \\
 m_3 & = \frac{\mu_n + \xi}{\mu_d}, \quad D = \frac{d c \xi}{\mu_d}.
 \end{aligned}$$

Here, note that only  $m_1$  contains  $\alpha$  which is usually treated as a bifurcation parameter. Using the parameter values given in Table 1 we have

$$\mu_1 = \frac{25\sqrt{6}}{4}[A], \quad \mu_2 = \frac{2 \times 10^5}{3}[R_n],$$

$$\mu_3 = \frac{2 \times 10^5}{3}[R_d], \quad \mu_4 = \frac{1}{5} / \text{day},$$

which agree with the units of the state variables and time. Moreover, assuming  $\alpha = \frac{1}{2000} = 0.0005$ , we have the new parameters which are indeed dimensionless, given by

$$m_1 = \frac{50}{9} \approx 5.555556, \quad m_2 = \frac{9}{4} = 2.25,$$

$$m_3 = \frac{5}{8} = 0.625, \quad D = 2. \quad (36)$$

It is easy to obtain two equilibrium solutions from (35) as follows:

$$E_0 : (0, 0, 0),$$

$$E_1 : \left( \sqrt{\frac{m_3(m_1 - m_2)}{1 + D}}, \frac{m_1 - m_2}{1 + D}, \frac{m_1 - m_2}{1 + D} \right),$$

$$(m_1 \geq m_2). \quad (37)$$

A simple linear analysis based on the Jacobian of (35) shows that when  $m_1 < m_2$ , the disease-free equilibrium  $E_0$  is stable while the disease equilibrium  $E_1$  does not exist; when  $m_1 > m_2$ ,  $E_0$  becomes unstable and  $E_1$  emerges. The characteristic polynomial for  $E_1$  is given by

$$P_1(\lambda) = \lambda^3 + (1 + m_3)\lambda^2$$

$$+ \frac{m_3[1 + D + 2(m_1 - m_2)]}{1 + D}\lambda$$

$$+ 2m_3(m_1 - m_2), \quad (38)$$

indicating that  $m_1 = m_2$  defines a transcritical bifurcation point between  $E_0$  and  $E_1$ , and there is no static bifurcation from  $E_1$  when  $m_1 > m_2$ .

$$\frac{\partial \alpha}{\partial m_1}(m_{1H}) = \frac{m_3(D - m_3)^2}{(1 + D)[D(1 + m_3) + m_3(m_3 + 2)(D - m_3)]} > 0.$$

Next, introducing the following affine transformation

$$\begin{pmatrix} X \\ Y \\ Z \end{pmatrix} = \begin{pmatrix} \sqrt{\frac{m_3(m_1 - m_2)}{1 + D}} \\ \frac{m_1 - m_2}{1 + D} \\ \frac{m_1 - m_2}{1 + D} \end{pmatrix} + P \begin{pmatrix} x_1 \\ x_2 \\ x_3 \end{pmatrix}, \quad (40)$$

As a matter of fact, we can treat  $m_1 - m_2$  as a single parameter and thus the transcritical bifurcation point becomes  $m_1 - m_2 = 0$ , and in fact the formulas given below on the analysis of Hopf bifurcation indeed does not involve the parameter  $m_2$  if we choose  $m_1$  as the perturbation parameter for the Hopf bifurcation.

Therefore, the only possible bifurcation from  $E_1$  is Hopf bifurcation. The critical Hopf bifurcation point is determined by the condition,  $\Delta_2 = 0$ , where

$$\Delta_2 = (1 + m_3) \frac{m_3[1 + D + 2(m_1 - m_2)]}{1 + D}$$

$$- 2m_3(m_1 - m_2)$$

$$= \frac{m_3}{1 + D} [2(m_1 - m_2)(m_3 - D)$$

$$+ (1 + D)(1 + m_3)].$$

It is easy to see that when  $m_1 > m_2$  and  $m_3 - D > 0$ ,  $E_1$  is always stable, and a Hopf bifurcation occurs from  $E_1$  only if  $m_3 < D$ . Hence, the Hopf critical point is defined by

$$m_{1H} = m_2 + \frac{(1 + D)(1 + m_3)}{2(D - m_3)}, \quad (D > m_3), \quad (39)$$

where the subcritical H denotes Hopf bifurcation. Further, suppose the characteristic polynomial equation  $P_1(\lambda) = 0$  has one real eigenvalue  $\lambda_1(m_1)$  and a complex conjugate,  $\lambda_{2,3}(m_1) = \alpha(m_1) \pm i\omega(m_1)$ . It should be noted that  $\lambda(m_1)$ ,  $\alpha(m_1)$  and  $\omega(m_1)$  contain other parameters  $m_2$ ,  $m_3$  and  $D$ . Then, at this critical point  $m_1 = m_{1H}$ , we have

$$\lambda_1(m_{1H}) = -(1 + m_3) < 0, \quad \alpha(m_{1H}) = 0 \quad \text{and}$$

$$\omega(m_{1H}) = \omega_c = \sqrt{\frac{m_3(1 + D)}{D - m_3}} > 0, \quad (D > m_3).$$

Moreover, we can show that the transversal condition is satisfied:

where

$$P = \begin{bmatrix} -\omega_c \sqrt{\frac{1+m_3}{2(1+D)}} & \sqrt{\frac{(1+D)(1+m_3)}{2}} & \frac{m_3}{\omega_c} \sqrt{\frac{1+D}{2(1+m_3)}} \\ 1 & \omega_c & -m_3 \\ 1 & 0 & 1 \end{bmatrix},$$

into system (35) we obtain

$$\begin{aligned} \frac{dx_1}{d\tau} &= \omega_c x_2 + \frac{1}{2C_1} [-m_3(1+m_3)C_9 x_1^2 + (1+D)(1+m_3)C_6 x_2^2 + 3m_3(D-m_3)^2 x_3^2 \\ &\quad + 2\omega_c(1+m_3)C_4 x_1 x_2 + 2m_3(D-m_3)x_1 x_3 + 2\omega_c(D-m_3)C_5 x_2 x_3], \\ \frac{dx_2}{d\tau} &= -\omega_c x_1 + \frac{1}{2C_1} \left[ \omega_c(1+m_3)C_5 x_1^2 + \omega_c(1+m_3)(D-m_3)C_8 x_2^2 - \frac{\omega_c(D-m_3)^2 C_2}{(1+D)(1+m_3)} x_3^2 \right. \\ &\quad \left. - 2(1+m_3)(D-m_3)C_7 x_1 x_2 - \frac{2m_3 C_3}{\omega_c} x_1 x_3 - 2(D-m_3)^2 C_{10} x_2 x_3 \right], \\ \frac{dx_3}{d\tau} &= -(1+m_3)x_3 + \frac{1}{2C_1} [m_3(1+m_3)C_9 x_1^2 - (1+D)(1+m_3)C_6 x_2^2 - 3m_3(D-m_3)^2 x_3^2 \\ &\quad - 2\omega_c(1+m_3)C_4 x_1 x_2 - 2m_3(D-m_3)C_8 x_1 x_3 - 2\omega_c(D-m_3)C_5 x_2 x_3], \end{aligned} \tag{41}$$

where

$$\begin{aligned} C_1 &= D(1+m_3) + m_3(m_3+2)(D-m_3), & C_2 &= (2m_3^2 + 3m_3 + 2)(D-m_3) - m_3(1+m_3), \\ C_3 &= 2(Dm_3 - m_3^2 + D)(D-m_3) + m_3(1+m_3), & C_4 &= (D-m_3)^2 - m_3, \\ C_5 &= (1+2m_3)(D-m_3) + D, & C_6 &= m_3(D-m_3) + D + m_3, \\ C_7 &= D(1+m_3) + 1 + 2m_3, & C_8 &= D - 1 - 2m_3, \\ C_9 &= 2D + 1 - m_3, & C_{10} &= 1 + m_3 + m_3^2. \end{aligned} \tag{42}$$

Indeed the system (41) does not involve the parameter  $m_2$ , as expected.

Next, we briefly explain how to use the method of normal forms to study bifurcation of multiple limit cycles. Suppose the general nonlinear differential system we are considering is given by  $\dot{\mathbf{x}} = J\mathbf{x} + \mathbf{f}(\mathbf{x})$ , where  $J\mathbf{x}$  and  $\mathbf{f}(\mathbf{x})$  represent the linear and nonlinear parts of the system, respectively. We assume  $\mathbf{f}$  is analytic and  $\mathbf{f}(\mathbf{0}) = \mathbf{0}$ , implying that  $\mathbf{x} = \mathbf{0}$  is an equilibrium point of the system, and  $J$  is the Jacobian of the system evaluated at the equilibrium point  $\mathbf{x} = \mathbf{0}$ . Further suppose  $J$  contains a purely imaginary pair and its other eigenvalues have negative real part. Then, by applying normal form theory, we can obtain the normal form (17), where  $v_k$  and  $\tau_k$  are explicitly expressed in terms

of the original system's coefficients.  $v_k$  is called the  $k$ th-order focus value of the Hopf-type critical point (the origin).

The basic idea of finding  $k$  small-amplitude limit cycles of the system  $\dot{\mathbf{x}} = J\mathbf{x} + \mathbf{f}(\mathbf{x})$  around the origin is as follows: First, find the conditions such that  $v_0 = v_1 = \dots = v_{k-1} = 0$  (note that  $v_0 = 0$  is automatically satisfied at the critical point), but  $v_k \neq 0$ , and then perform appropriate small perturbations to prove the existence of  $k$  limit cycles. The following lemma gives sufficient conditions for the existence of small-amplitude limit cycles. (The proof can be found in [Yu & Han, 2005].)

**Lemma 2.** *Suppose that the focus values of a dynamical system depend on  $k$  parameters, expressed*

as

$$v_j = v_j(\epsilon_1, \epsilon_2, \dots, \epsilon_k), \quad j = 0, 1, \dots, k, \quad (43)$$

satisfying

$$\begin{aligned} v_j(0, \dots, 0) = 0, \quad j = 0, 1, \dots, k-1, \\ v_k(0, \dots, 0) \neq 0 \end{aligned} \quad (44)$$

and

$$\det \left[ \frac{\partial(v_0, v_1, \dots, v_{k-1})}{\partial(\epsilon_1, \epsilon_2, \dots, \epsilon_k)}(0, \dots, 0) \right] \neq 0.$$

Then, for any given  $\epsilon_0 > 0$ , there exist  $\epsilon_1, \epsilon_2, \dots, \epsilon_k$  and  $\delta > 0$  with  $|\epsilon_j| < \epsilon_0$ ,  $j = 1, 2, \dots, k$  such that the equation  $\dot{r} = 0$  has exactly  $k$  real positive roots for  $r$  (i.e. the dynamical system has exactly  $k$  limit cycles) in a  $\delta$ -ball with the center at the origin.

Now we apply the Maple program developed in [Yu, 1998] for computing the normal forms of Hopf and generalized Hopf bifurcation to system (41) to obtain

$$\begin{aligned} v_1 &= -\frac{Dm_3(1+m_3)^2(D-m_3)(1+D-m_3)}{C_1^2[D(m_3^2+6m_3+1)+m_3(1-m_3)(3+m_3)]} \\ &\quad \times [3(1+m_3)D^2 - (7m_3^2+6m_3+1)D + m_3(4m_3^2+5m_3+3)], \\ v_2 &= v_2(D, m_3) = \dots, \\ v_3 &= v_3(D, m_3) = \dots, \end{aligned}$$

where  $C_1$  is given in (42), and the lengthy expressions of  $v_2$  and  $v_3$  are omitted here for brevity. It is seen that the focus values only contain two parameters  $D$  and  $m_3$ , and so in general, we may obtain three limit cycles by using  $D$  and  $m_3$  to solve  $v_1 = v_2 = 0$  but  $v_3 \neq 0$ . To achieve this, eliminating  $D$  from the equations  $v_1 = v_2 = 0$  yields a solution  $D = D(m_3)$  and one resultant  $R_{12}$ , given by

$$\begin{aligned} R_{12} &= m_3(m_3+1)(m_3^2+4m_3+1)(m_3^2+14m_3+1) \\ &\quad \times (64260m_3^{16} + 11622021m_3^{15} + 145525211m_3^{14} + 938104849m_3^{13} + 4533531166m_3^{12} \\ &\quad + 16130725479m_3^{11} + 40116273317m_3^{10} + 69028372739m_3^9 + 82632778940m_3^8 \\ &\quad + 69028372739m_3^7 + 40116273317m_3^6 + 16130725479m_3^5 + 4533531166m_3^4 \\ &\quad + 938104849m_3^3 + 145525211m_3^2 + 11622021m_3 + 64260). \end{aligned}$$

It is obvious that  $R_{12} = 0$  has no positive solution for  $m_3$ , implying that we cannot have solutions for  $v_1 = v_2 = 0$ , and thus three limit cycles are not possible. The next best possibility is to have  $v_1 = 0$ , but  $v_2 \neq 0$ , yielding two small-amplitude limit cycles. Note that using the values of  $m_2, m_3$  and  $D$  given in (36) we have  $m_{1H} = \frac{177}{44} \approx 4.022727$ , and  $v_1 \approx -0.149119$ . In order to have solutions for  $v_1 = 0$ , we solve the factor in the square bracket in the expression of  $v_1$  for  $D$  to obtain

$$\begin{aligned} D_{\pm} &= \frac{1}{6(1+m_3)} [1 + 6m_3 + 7m_3^2 \\ &\quad \pm \sqrt{m_3^4 - 24m_3^3 - 46m_3^2 - 24m_3 + 1}]. \end{aligned} \quad (45)$$

It is easy to see that  $D_{\pm} > 0$  provided the following condition is satisfied:

$$\begin{aligned} m_3^4 - 24m_3^3 - 46m_3^2 - 24m_3 + 1 &\geq 0 \\ \Leftrightarrow m_3 \leq 0.038733 \dots \quad \text{or} \quad m_3 &\geq 25.817673 \dots \end{aligned}$$

We take  $m_3 = 0.035$ ,  $m_2 = 2.25$ , and  $D = D_+ = 0.247813 \dots$ , for which  $v_1 = 0$  and  $v_2 \approx -0.019355$ . Thus, by Lemma 2 we can conclude that system (35) can have two small-amplitude limit cycles near the equilibrium solution  $E_1$  due to Hopf bifurcation.

Summarizing the above results we have the following theorem.

**Theorem 3.** *The system (35) has two equilibrium solutions  $E_0$  and  $E_1$ .  $E_0$  is a stable node for  $m_1 < m_2$  and becomes a saddle for  $m_1 > m_2$ .  $E_0$  loses its stability at the transcritical point  $m_1 = m_2$ , at which the equilibrium  $E_1$  emerges and exist for  $m_1 > m_2$ .*

$E_1$  is asymptotically stable for  $m_1 \in (m_2, m_{1H})$ , where  $m_{1H}$  is a Hopf critical point. There does not exist conditions such that both the first and second focus values vanish, and at the critical value  $D = D_+$ ,  $v_1 = 0$  and  $v_2 \neq 0$ , for which proper perturbations can be chosen for system (35) to exhibit two small-amplitude limit cycles.

Note in Theorem 3 that in order to obtain two small-amplitude limit cycles, the values of  $D$  and  $m_3$  are chosen much smaller than that given in (30). To realize the two limit cycles, with  $m_2 = 2.25$  and  $m_3 = 0.035$ , we take perturbations on  $D$  and  $m_1$  as  $D = D_+ - 0.05$ , where  $m_1 = m_{1H} - 0.0001$ , and so the focus values become

$$v_0 \approx -0.181712 \times 10^{-6}, \quad v_1 \approx 0.361977 \times 10^{-3}, \\ v_2 \approx -0.018333.$$

Thus, the truncated normal form equation  $\dot{r} = v_0 + v_1 r^2 + v_2 r^4 = 0$  yields the approximations for the amplitudes of the two limit cycles:  $r_1 \approx 0.022704$  and  $r_2 \approx 0.138669$ . Since  $v_0 < 0$  and  $v_2 < 0$ , the equilibrium point  $E_1 : (X, Y, Z) = (0.333532, 3.178398, 3.178398)$  and the outer limit cycle are stable, while the inner limit cycle is unstable due to  $v_1 > 0$ . This is indeed a bistable phenomenon consisting of a stable equilibrium and a stable limit cycle. If restricted to the center manifold, the unstable limit cycle is a separatrix for the two attracting regions. In the three-dimensional space, trajectories converge to either the stable equilibrium or the stable limit cycle.

However, it should be noted that here we are looking for only two limit cycles, and hence, we do not necessarily follow Lemma 2, which gives a sufficient condition for the existence of small-amplitude limit cycles. As long as under proper perturbation, we can find two positive roots from the equation:  $v_0 + v_1 r^2 + v_2 r^4 = 0$ , and higher-order focus values are small, then two small-amplitude limit cycles are obtained. Thus, we may take certain perturbations such that  $v_2$  changes from negative to positive. For example, since  $D$  is allowed to take larger values, we choose  $D = 0.747814$  and  $m_1 \approx 3.528906$ , for which the focus values become

$$v_0 \approx 0.000036, \quad v_1 \approx -0.023369, \quad v_2 \approx 0.219378.$$

Thus solving the equation  $v_0 + v_1 r^2 + v_2 r^4 = 0$  yields two positive roots:  $r_1 \approx 0.039603$  and  $r_2 \approx 0.323967$ , which approximate the amplitudes of the bifurcating limit cycles. Moreover, the inner limit

cycle is stable and the outer one is unstable. For this case,  $v_0 > 0$  and  $v_2 > 0$ , so the equilibrium point  $E_1 : (X, Y, Z) = (0.160032, 0.731718, 0.731718)$  and the outer limit cycle are unstable, while the inner limit cycle is stable because of  $v_1 < 0$ . Hence, for this case the system does not exhibit bistable phenomenon, and all solution trajectories converge to the stable limit cycle.

Numerical simulation for one of the above two cases will be given in the next section.

## 5. Numerical Simulations

In this section, numerical simulations are presented to compare with the analytical predictions obtained in the previous sections. In particular, the comparison between the analytical and numerical results obtained for the Hopf and generalized Hopf bifurcations is given. In order to give a good comparison, for Hopf bifurcation we fix all parameter values, but  $\alpha$  (or  $\mu$ ), which is treated as a bifurcation parameter. The parameter  $\alpha$  is varied to show the stable equilibrium solutions  $E_0$  and  $E_1$ , and stable limit cycles. Moreover, we will choose a large positive value of  $\mu$ , which means that this value is far away from the Hopf critical point  $\alpha_H$ , to demonstrate the blips phenomenon. While for the generalized Hopf bifurcation, we use the dimensionless system (35) and, besides the parameter  $m_1$  treated as a bifurcation parameter (which is a function of  $\alpha$ ), we take  $D$  as the second perturbation parameter.

Having taken all parameter values, except for  $\alpha$ , from Table 1, it follows from Lemma 1 that the disease-free equilibrium  $E_0$  is asymptotically stable for  $0 < \alpha < \alpha_t = 0.2025 \times 10^{-3}$ . Then, as  $\alpha$  is increased to pass through  $\alpha_t$ ,  $E_0$  becomes unstable and bifurcates into the disease equilibrium  $E_1$ , which is asymptotically stable for  $\alpha_t < \alpha < \alpha_H = 0.7867 \times 10^{-3}$ . As  $\alpha$  is further increased,  $E_1$  becomes unstable at the Hopf critical point  $\alpha = \alpha_H$ , leading to a family of limit cycles. The normal form obtained for the Hopf bifurcation is given in (27). Since  $v_1 = -0.2016072570 \times 10^{-11} < 0$ , the Hopf bifurcation is supercritical, and the bifurcating limit cycles are stable.

To show the series of bifurcations, we vary the bifurcation parameter  $\alpha$  and increase its value from a small one less than  $\alpha_t$ . We first choose  $\alpha = 0.15 \times 10^{-3} < \alpha_t$ , with the simulation result shown in Fig. 2, indicating that  $E_0$  is asymptotically stable, which agrees with the analytical prediction. Next, choose  $\alpha_t < \alpha = 0.4 \times 10^{-3} < \alpha_H$ , with the

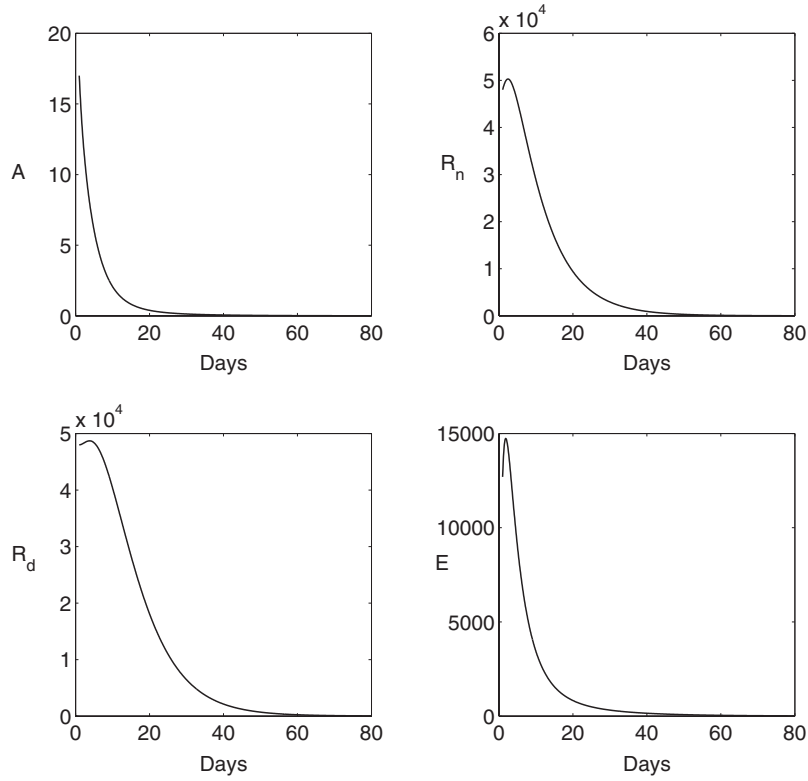


Fig. 2. Simulated time history for system (1) when  $\alpha = 0.15 \times 10^{-3} < \alpha_t$ , with the initial condition  $A(0) = 17$ ,  $R_n(0) = R_d(0) = 48\,000$ ,  $E(0) = 12\,700$ , converging to  $E_0$ .

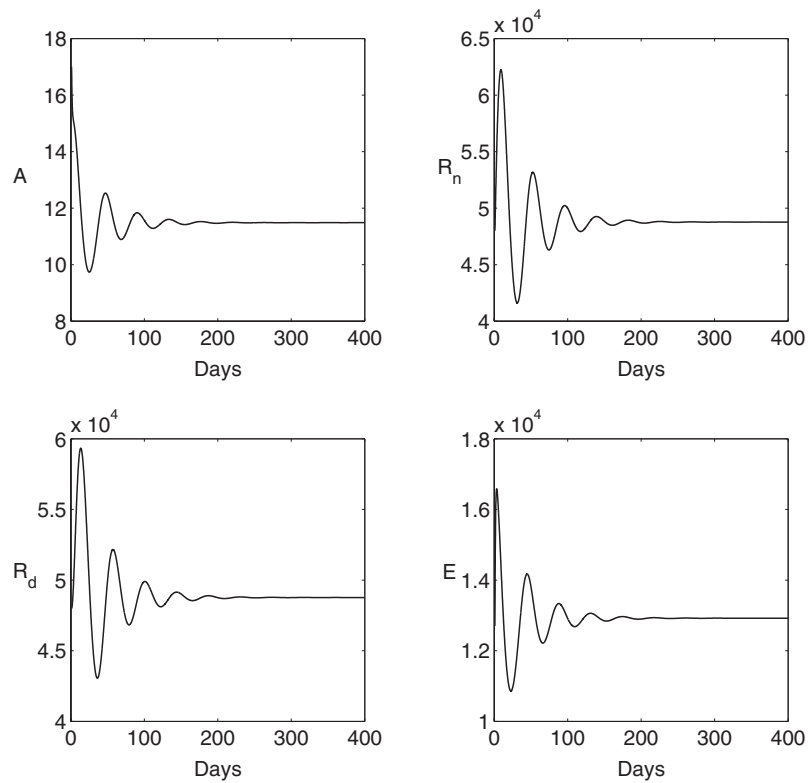


Fig. 3. Simulated time history for system (1) when  $\alpha = 0.4 \times 10^{-3}$ , with the initial condition,  $A(0) = 17$ ,  $R_n(0) = R_d(0) = 48\,000$ ,  $E(0) = 12\,700$ , converging to  $E_1$ .

simulation result depicted in Fig. 3, showing that  $E_1$  is asymptotically stable, which again agrees with the analytical prediction. For  $\alpha > \alpha_H$ , we select two values of  $\mu = 0.3 \times 10^{-11}$  and  $\mu = 0.1 \times 10^{-10}$ , both of which are near the Hopf bifurcation point, implying two perfect Hopf bifurcations. In order to compare the simulation results with the analytical

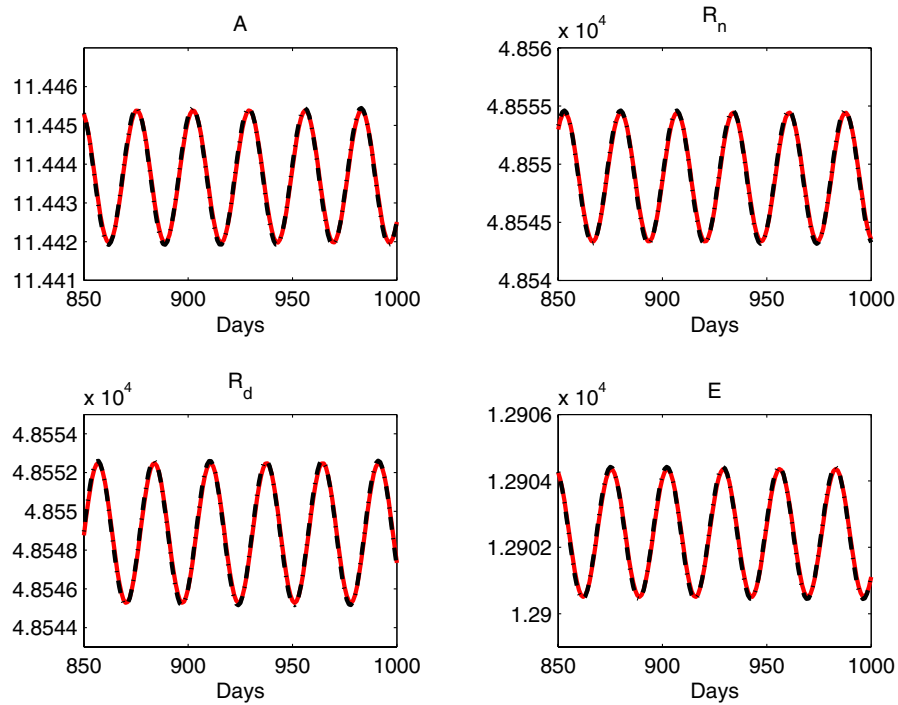
predictions for the two Hopf bifurcations, we use the sliding and parameter transformation (23), then apply the normal form (27), the limit cycle solutions (29) and (30), and the output (32) from executing the Maple program [Yu, 1998] to obtain the following analytical approximations:

For  $\mu = 0.3 \times 10^{-11}$ ,

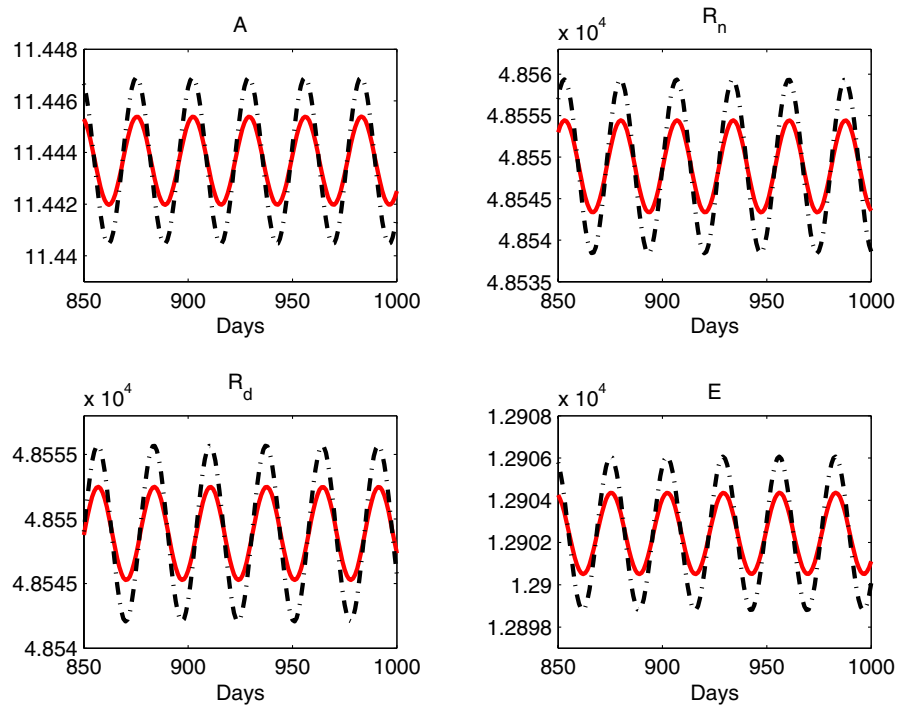
$$\begin{aligned}
 A(t) &= 11.44368258 + 0.46972 \times 10^{-11} \cos(0.70065t) + 0.51885 \times 10^{-12} \sin(0.70065t) \\
 &\quad - 0.83409 \times 10^{-3} \cos(0.23355t) + 0.15584 \times 10^{-2} \sin(0.23355t) \\
 &\quad - 0.46083 \times 10^{-7} \cos(0.46710t) - 0.84711 \times 10^{-7} \sin(0.46710t), \\
 R_n(t) &= 48548.88564 + 0.16404 \times 10^{-8} \cos(0.70065t) + 0.12499 \times 10^{-7} \sin(0.70065t) \\
 &\quad - 5.7426 \cos(0.23355t) + 0.34563 \times 10^{-8} \sin(0.23355t) \\
 &\quad + 0.18602 \times 10^{-3} \cos(0.46710t) - 0.18823 \times 10^{-3} \sin(0.46710t), \\
 R_d(t) &= 48548.88564 - 0.31754 \times 10^{-8} \cos(0.70065t) + 0.13747 \times 10^{-8} \sin(0.70065t) \\
 &\quad - 2.4296 \cos(0.23355t) - 2.8372 \sin(0.23355t) \\
 &\quad + 0.96927 \times 10^{-4} \cos(0.46710t) + 0.38148 \times 10^{-4} \sin(0.46710t), \\
 E(t) &= 12902.43192 + 0.52959 \times 10^{-8} \cos(0.70065t) + 0.58498 \times 10^{-9} \sin(0.70065t) \\
 &\quad - 0.94041 \cos(0.23355t) + 1.7570 \sin(0.23355t) \\
 &\quad - 0.51957 \times 10^{-4} \cos(0.46710t) - 0.95508 \times 10^{-4} \sin(0.46710t).
 \end{aligned} \tag{46}$$

For  $\mu = 0.1 \times 10^{-10}$ ,

$$\begin{aligned}
 A(t) &= 11.44368267 + 0.28584 \times 10^{-10} \cos(0.70065t) + 0.31574 \times 10^{-11} \sin(0.70065t) \\
 &\quad - 0.15228 \times 10^{-2} \cos(0.23355t) + 0.28452 \times 10^{-2} \sin(0.23355t) \\
 &\quad - 0.15361 \times 10^{-6} \cos(0.46710t) - 0.28237 \times 10^{-6} \sin(0.46710t), \\
 R_n(t) &= 48548.88610 + 0.99821 \times 10^{-8} \cos(0.70065t) + 0.76060 \times 10^{-7} \sin(0.70065t) \\
 &\quad - 10.484 \cos(0.23355t) + 0.21032 \times 10^{-7} \sin(0.23355t) \\
 &\quad + 0.62007 \times 10^{-3} \cos(0.46710t) - 0.62742 \times 10^{-3} \sin(0.46710t), \\
 R_d(t) &= 48548.88610 - 0.19324 \times 10^{-7} \cos(0.70065t) + 0.83652 \times 10^{-8} \sin(0.70065t) \\
 &\quad - 4.4358 \cos(0.23355t) - 5.1798 \sin(0.23355t) \\
 &\quad + 0.32309 \times 10^{-3} \cos(0.46710t) + 0.12716 \times 10^{-3} \sin(0.46710t), \\
 E(t) &= 12902.43196 + 0.32227 \times 10^{-7} \cos(0.70065t) + 0.35598 \times 10^{-8} \sin(0.70065t) \\
 &\quad - 1.7169 \cos(0.23355t) + 3.2078 \sin(0.23355t) \\
 &\quad - 0.17319 \times 10^{-3} \cos(0.46710t) - 0.31836 \times 10^{-3} \sin(0.46710t).
 \end{aligned} \tag{47}$$



(a)



(b)

Fig. 4. Comparison between the simulated time history and analytical approximations for system (1), the red solid line denoting the simulation results, while the black dash-dot line indicating the analytical predictions. The bifurcation parameter values of  $\mu$  are taken for two cases: (a)  $\mu = 0.3 \times 10^{-11}$  and (b)  $\mu = 0.1 \times 10^{-10}$ , both converging to stable limit cycles.

The two sets of simulation results compared with the above two sets of analytical solutions are shown in Fig. 4. It clearly shows a very good agreement between the simulation results and the analytical predictions, particularly for the smaller value of  $\mu$ , as expected. The comparison result for  $\mu = 0.3 \times 10^{-11}$  has been given in [Zhang *et al.*, 2014], but the detailed analytical formulas are not given there. To demonstrate the blips phenomenon, we choose a value of  $\alpha = 0.3 \times 10^{-2} > \alpha_H$ , which is not close to  $\alpha_H$ , and so the normal form theory is not applicable for this value. The simulation result for this case is given in Fig. 5, indeed showing the blips phenomenon. Since the solutions of the system are positive and bounded, and the Hopf bifurcation induces oscillations, we expect that the system can have large-amplitude oscillating solutions (a persistent motion), and choosing appropriate parameter values can tune the frequency of the motion to become blips. The biological reason for the model to exhibit blips is as follows (see Fig. 5): the variable  $E$  grows very quickly in the absence of the variables  $R_n$  and  $R_d$ , and then  $R_n$  responds very quickly (due to the  $EA$  term) and suppresses the  $E$ , but the  $R_n$  does not last long. This explains how the

adaptive and innate immune responses work too, against pathogens. But why is the  $E$  not eliminated like a pathogen would be? Maybe because the system is now “torn between two equilibria”.

Finally, we present simulations for the bifurcation of two limit cycles obtained in the previous section. We consider the case with  $v_2 > 0$ , for which the parameter values are given by

$$\begin{aligned} m_2 &= 2.25, & m_3 &= 0.035, \\ m_1 &= 3.52890612, & D &= 0.74781360. \end{aligned} \tag{48}$$

We use the normalized system (35) to perform the simulation. The simulations are shown in Fig. 6, with the equilibrium  $E_1$  given at  $(X, Y, Z) = (0.1600, 0.7317, 0.7317)$ . Figures 6(a)–6(d) show the convergence to the small limit cycle from different initial points, and in particular, a different scale is used in Fig. 6(a) to show a zoomed region where a trajectory (with dots plotting) starting from an initial point close to the equilibrium  $E_1$  converges to the limit cycle. Note that at the equilibrium point  $E_1$ , the eigenvalues have a negative eigenvalue and a pair of complex conjugate with very small positive real part. Thus  $E_1$  becomes a focus-saddle. Because

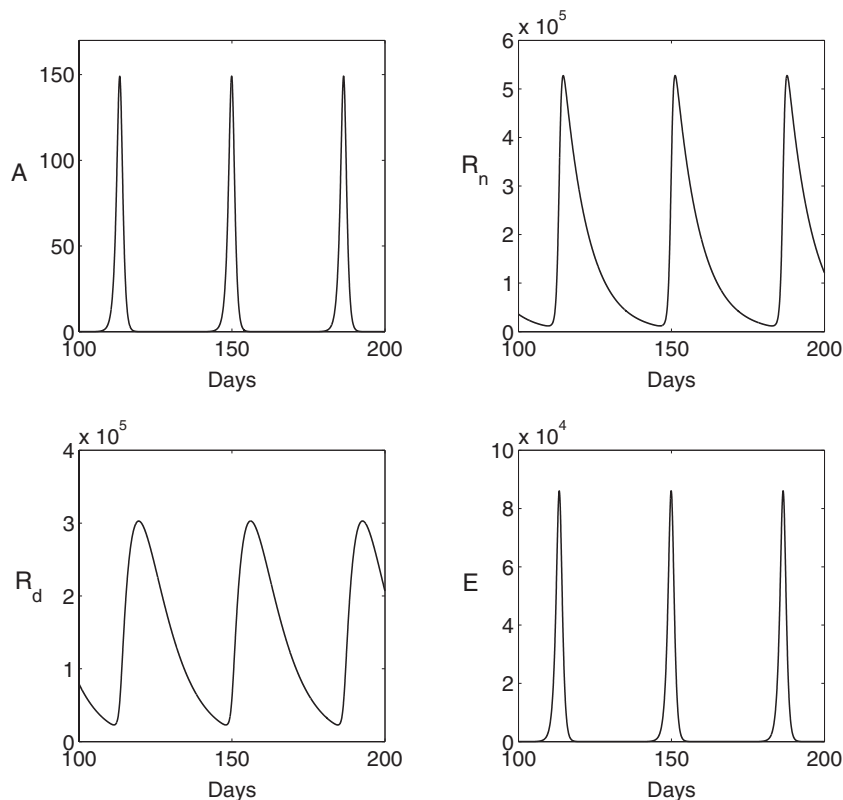


Fig. 5. Simulated time history for system (1) when  $\alpha = -0.3 \times 10^{-2}$ , showing blips.

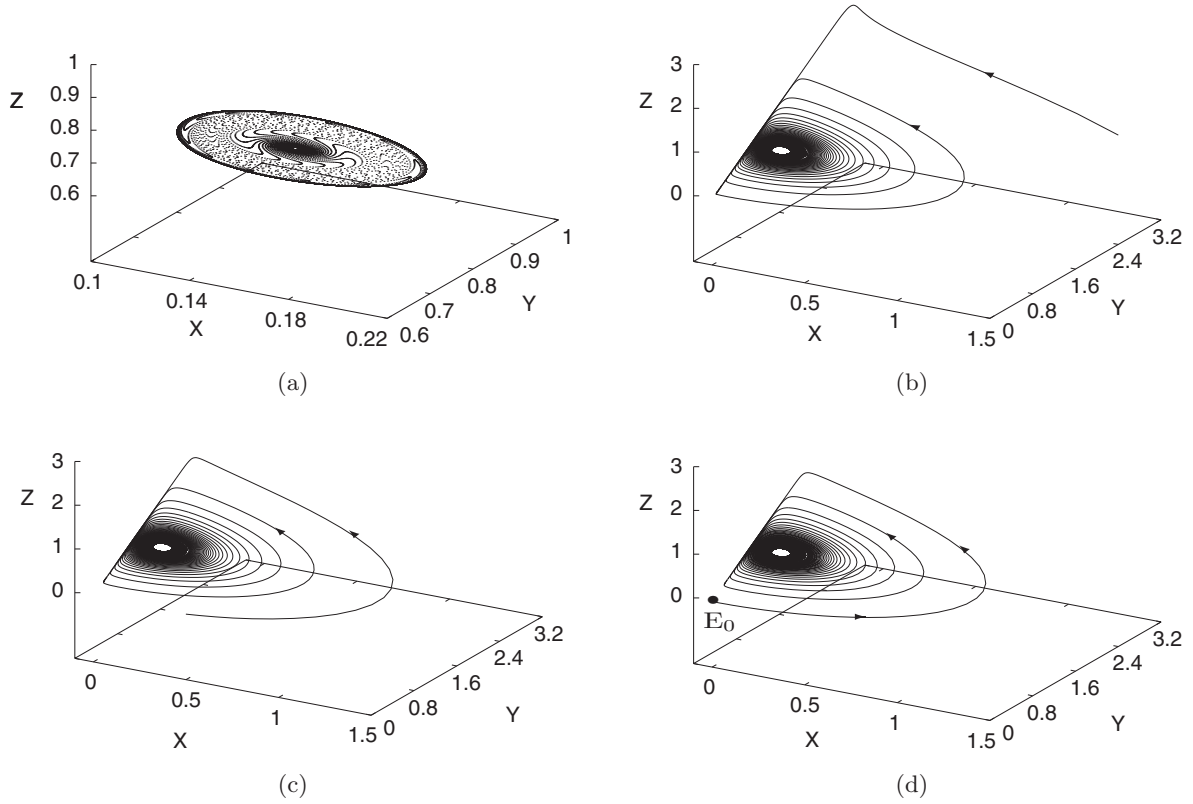


Fig. 6. Simulated trajectories of system (35) for  $m_1 = 3.52890612$ ,  $m_2 = 2.25$ ,  $m_3 = 0.035$ ,  $D = 0.74781360$ , all of them converging to the small limit cycle, with the initial points taken at (a)  $(X, Y, Z) = (0.16, 0.73, 0.73)$ , (b)  $(X, Y, Z) = (1.5, 2.4, 1)$ , (c)  $(X, Y, Z) = (0.5, 0, 0)$  and (d)  $(X, Y, Z) = (0.000001, 0, 0)$ .

$E_0$  is a saddle, there must exist a separatrix connecting  $E_0$  and  $E_1$ , and the trajectory starting from  $E_0$  on the unstable part converges to  $E_1$  as  $t \rightarrow +\infty$ .

The two limit cycles are located on a center manifold which passes through the equilibrium  $E_1$ . In order to show the unstable limit cycle, we restrict the system to the center manifold, which is obtained

by assuming the center manifold expanded in the form of  $x_3 = x_3(x_1, x_2) = a_{20}x_1^2 + a_{11}x_1x_2 + a_{02}x_2^2 + \dots$  (up to fifth-order) and then using system (35) to determine the undetermined coefficients  $a_{ij}$ . Then, transferring the form back to the original variables  $X, Y, Z$  we obtain the following equation:

$$\begin{aligned}
 \text{CM} = & -0.0683915894 + 0.2016906273X - 0.8793688885Y + 0.9470797978Z + 0.0622322204X^2 \\
 & - 0.0664272886Y^2 + 0.0004776377Z^2 + 0.0497178205XY - 0.0119240109XZ \\
 & - 0.0101081034YZ + 0.0733485001X^3 + 0.0425268638Y^3 - 0.0001740782Z^3 \\
 & - 0.1622094496X^2Y - 0.0298346829X^2Z + 0.0775152987XY^2 - 0.0040445755Y^2Z \\
 & + 0.0039935873XZ^2 - 0.0023944203YZ^2 + 0.0410418940XYZ + \dots \\
 = & 0.
 \end{aligned} \tag{49}$$

The graph of the center manifold is depicted in Fig. 7(a), which seems very close to a plane near the equilibrium  $E_1$ . For the given parameter values in (48), we obtain the following differential equations up to fifth-order, describing the dynamics on the center manifold:

$$\begin{aligned}
 \frac{dx_1}{d\tau} = & 0.000036x_1 + 0.292950x_2 - 0.054038x_1^2 + 0.173926x_1x_2 + 0.054038x_2^2 - 0.000034x_1^3 \\
 & + 0.003022x_1^2x_2 - 0.065757x_1x_2^2 - 0.001346x_2^3 + 0.000110x_1^4 - 0.002335x_1^3x_2 - 0.078314x_1^2x_2^2
 \end{aligned}$$

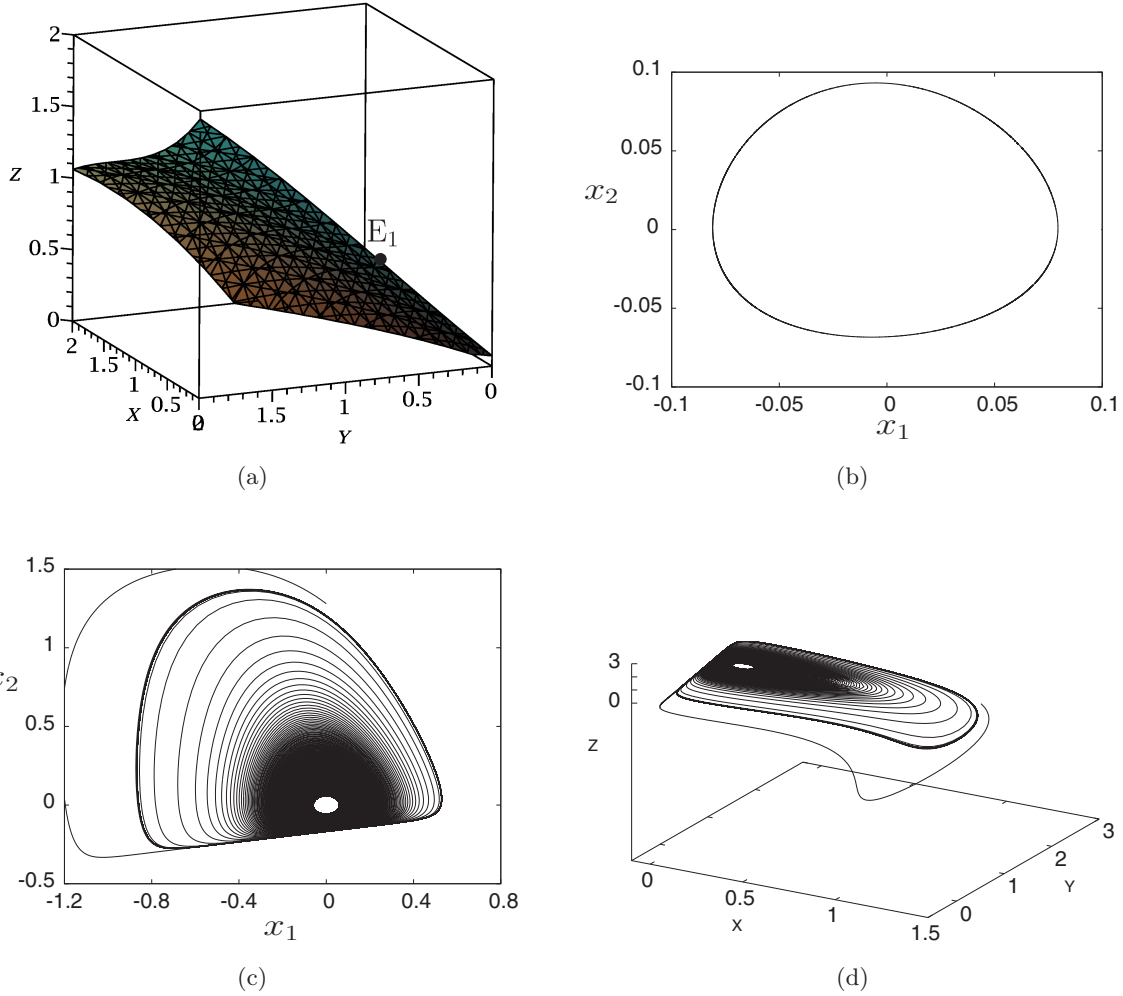


Fig. 7. (a) Center manifold (49), (b) simulated small limit cycle restricted to the center manifold based on the reduced system (50), (c) simulated large and small limit cycles near the manifold based on the reduced system (50) and (d) the simulation given in (c) transformed back to the original coordinate system.

$$\begin{aligned}
 & + 0.048821x_1x_2^3 - 0.010521x_2^4 - 0.000061x_1^5 + 0.003994x_1^4x_2 - 0.065173x_1^3x_2^2 + 0.167741x_1^2x_2^3 \\
 & - 0.112675x_1x_2^4 + 0.024607x_2^5, \\
 \frac{dx_2}{d\tau} = & -0.292950x_1 + 0.000036x_2 + 0.277655x_1^2 - 1.649484x_1x_2 - 0.277655x_2^2 - 0.000299x_1^3 \\
 & + 0.012383x_1^2x_2 + 0.110119x_1x_2^2 + 0.002246x_2^3 + 0.000952x_1^4 + 0.024591x_1^3x_2 + 0.117304x_1^2x_2^2 \\
 & - 0.078729x_1x_2^3 + 0.017561x_2^4 - 0.000507x_1^5 + 0.010039x_1^4x_2 + 0.063385x_1^3x_2^2 - 0.249426x_1^2x_2^3 \\
 & + 0.181397x_1x_2^4 - 0.041077x_2^5.
 \end{aligned} \tag{50}$$

The dynamics, in particular, the two limit cycles of the above reduced system are shown in Figs. 7(b) and 7(c). Note that now the origin of the reduced system is an unstable focus, corresponding to the original equilibrium  $E_0$ . The small stable limit cycle shown in Fig. 7(b) is obtained by using

the initial condition  $(x_1, x_2) = (0.0001, -0.0001)$ , converging to the limit cycle very slowly. Figure 7(c) shows both large and small limit cycles, and the outer unstable limit cycle is obtained by using the so-called “reversing time” simulation, that is,

simply take negative time step in a regular numerical integration scheme. Thus, trajectories diverging from the unstable limit cycles become converging to the limit cycle. But this approach is not applicable for dynamical systems which have dimension higher than two. The simulation given in Fig. 7(c) can be transformed back to the original coordinates  $(X, Y, Z)$  by using the center manifold transformation  $x_3 = x_3(x_1, x_2)$  as well as (47), as shown in Fig. 7(d).

The advantage of using the two-dimensional reduced dynamical system on the center manifold allows us to simulate the unstable limit cycle, which is difficult to do using the original three-dimensional system. A small drawback of this approach is that the center manifold (49) is not an exact or global expression, but an approximation. Hence, the trajectories not near the equilibrium  $E_1$  may have deviation from real solutions, and the deviation becomes large for the trajectories being far from the equilibrium. It can be seen from Fig. 7(b) that the small limit cycle has a very good approximation, compared with the analytical prediction  $r_1 \approx 0.04$ . However, it can be observed from Fig. 7(d) that the large limit cycle slightly reaches negative values, which are not allowed since the solutions of the original system (35) are positive provided the initial conditions are positive. But it is still good enough to confirm the analytic prediction, in particular for the unstable limit cycle, at least qualitatively.

## 6. Conclusion

In this paper, we have given a detailed study on an autoimmune model, particularly for bifurcation and stability properties. The main attention is focused on the dynamical oscillating behavior of the model, which may lead to the interesting and important phenomenon — blips. After finding two equilibrium solutions and their stability conditions, we have paid particular attention to Hopf bifurcation which may occur from the disease equilibrium, since Hopf bifurcation is a necessary condition to generate blips. We have applied center manifold theory and the method of normal forms to give a detailed analysis on the Hopf bifurcation. We have obtained the exact analytical formulas for the approximate solutions of limit cycles, which are compared with numerical simulations to show a very good agreement between the simulations and the analytical predictions.

Moreover, we have also investigated the bifurcation of multiple limit cycles, which can cause complex dynamics in biological systems such as bistable phenomenon which may involve stable equilibria and stable oscillating motions. We have particularly shown that the autoimmune model considered in this paper can indeed exhibit at least two limit cycles due to Hopf bifurcation. The results show that it is possible to have bistable phenomenon consisting of a stable equilibrium and an (outer) stable limit cycle, and the unstable small limit cycle, restricted to the center manifold, separates the attracting regions between the stable equilibrium and the stable limit cycle. Also, it is possible to have an (outer) unstable limit cycle and an inner stable limit cycle, both of them enclose an unstable limit cycle. In this case, there does not exist bistable phenomenon and all trajectories converge to the stable limit cycle.

The bifurcation of multiple cycles studied in this paper for an autoimmune model reveals that multiple limit cycle bifurcation may be one of the sources to yield complex dynamics in biological systems and can be used to realistically explain complex dynamics in real physical systems. The method developed in this paper can be easily extended to study other nonlinear dynamical systems. It is anticipated that this study may promote further researches in this field.

## Acknowledgment

This work was supported by the Natural Sciences and Engineering Research Council of Canada (No. R2686A02).

## References

- Alexander, H. K. & Wahl, L. M. [2011] “Self-tolerance and autoimmunity in a regulatory T cell model,” *Bull. Math. Biol.* **73**, 33–71.
- DeFranco, A., Locksley, R. & Robertson, M. [2007] *Immunity: The Immune Response to Infectious and Inflammatory Disease* (New Science Press Ltd., London).
- Farber, E. M., Mullen, R. H., Jacobs, A. H. & Nall, L. [1986] “Infantile psoriasis: A follow-up study,” *Pediatr. Dermat.* **3**, 237–243.
- Fergusson, D. M., Horwood, L. J. & Shannon, F. T. [1990] “Early solid feeding and recurrent childhood eczema: A 10-year longitudinal study,” *Pediatrics* **86**, 541–546.

- Field, E. H., Kulhankova, K. & Nasr, M. E. [2007] “Natural Tregs, CD4<sup>+</sup>CD25<sup>+</sup> inhibitory hybridomas, and their cell contact dependent suppression,” *Immunol. Res.* **39**, 62–78.
- Girschick, H. J., Zimmer, C., Klaus, G., Darge, K., Dick, A. & Morbach, H. [2007] “Chronic recurrent multifocal osteomyelitis: What is it and how should it be treated?” *Nat. Clin. Practice Rheumatol.* **3**, 733–738.
- Guckenheimer, J. & Holmes, P. [1990] *Nonlinear Oscillations, Dynamical Systems, and Bifurcations of Vector Fields*, 3rd edition (Springer-Verlag, NY).
- Hinrichsen, D. & Pritchard, A. J. [2005] *Mathematical Systems Theory I: Modelling, State Space Analysis, Stability and Robustness*, 2nd edition (Springer-Verlag, NY).
- Iyer, R. S., Thapa, M. M. & Chew, F. S. [2011] “Chronic recurrent multifocal osteomyelitis: Review,” *Amer. J. Roentgenol.* **196**, S87–S91.
- Miyara, M. & Sakaguchi, S. [2007] “Natural regulatory T cells: Mechanisms of suppression,” *Trends in Molecul. Med.* **13**, 108–116.
- Munro, D. D. [1963] “Recurrent subacute discoid lupus erythematosus,” *Proc. Roy. Soc. Med.* **56**, 78–79.
- Sakaguchi, S., Miyara, M., Costantino, C. M. & Hafler, D. A. [2010] “FOXP3<sup>+</sup> regulatory T cells in the human immune system,” *Nat. Rev. Immunol.* **10**, 490–500.
- Scheffold, A., Hühn, J. & Höfer, T. [2005] “Regulation of CD4<sup>+</sup>CD25<sup>+</sup> regulatory T cell activity: It takes (IL-) two to tango,” *European J. Immunol.* **35**, 1336–1341.
- Scheffold, A., Murphy, K. M. & Höfer, T. [2007] “Competition for cytokines: Treg cells take all,” *Nat. Immunol.* **8**, 1285–1287.
- Yu, P. [1998] “Computation of normal forms via a perturbation technique,” *J. Sound Vibr.* **211**, 19–38.
- Yu, P. [2003] “A simple and efficient method for computing center manifold and normal forms associated with semi-simple cases,” *Dyn. Contin., Discr. Impuls. Syst. Ser. B: Appl. Algorithm.* **10**, 273–286.
- Yu, P. [2005] “Closed-form conditions of bifurcation points for general differential equations,” *Int. J. Bifurcation and Chaos* **15**, 1467–1483.
- Yu, P. & Han, M. [2005] “Small limit cycles bifurcating from fine focus points in cubic-order  $z_2$ -equivariant vector fields,” *Chaos Solit. Fract.* **24**, 329–348.
- Zhang, W., Wahl, L. M. & Yu, P. [2014] “Modelling and analysis of recurrent autoimmune disease,” *SIAM J. Appl. Math.* **74**, 1998–2025.